Toward NNLO accuracy of parton distribution functions

Pavel Nadolsky

Southern Methodist University
Dallas, TX, U.S.A.

in collaboration with
M. Guzzi, F. Olness,
J. Huston, H.-L. Lai, Z. Li, J. Pumplin, C.-P. Yuan (CTEQ)

September 23, 2011

NNLO PDF sets as the new norm

- PDFs with NNLO (two-loop) QCD corrections to DIS and DY processes are becoming the standard. They are now produced by 6 groups.
- Our general-purpose set CT10 is obtained at NLO *(PRD82, 074024 (2010))*. The CT10.1 NNLO set undergoes pre-publication tests.

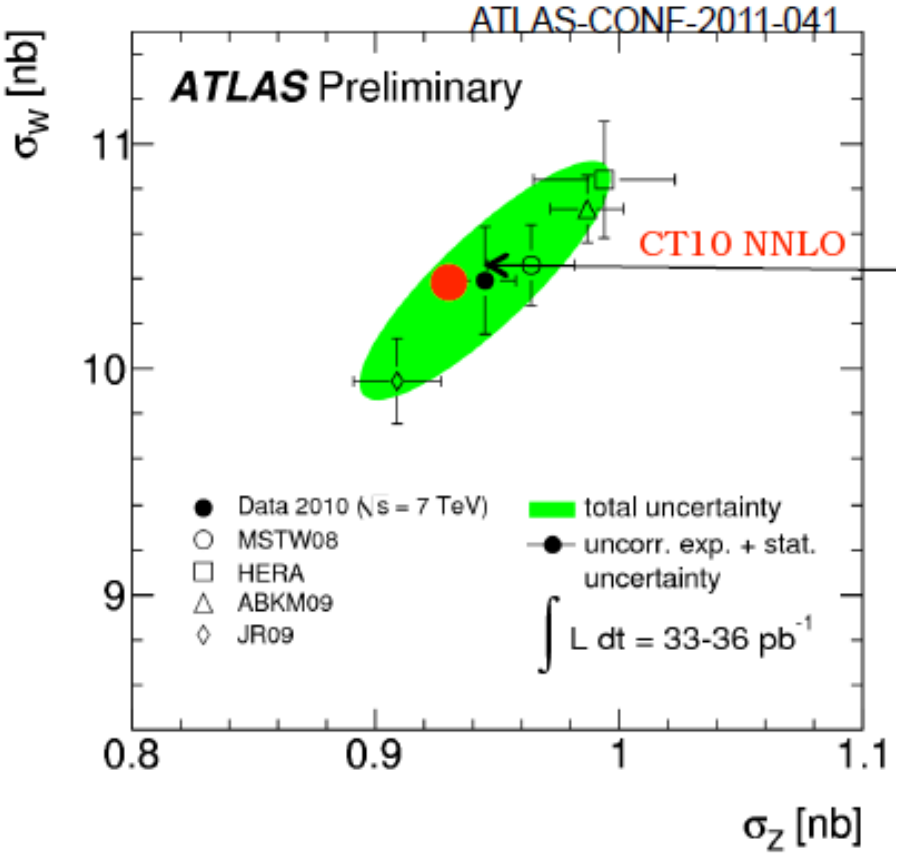

The agreement between NNLO PDF sets is not automatically better than at NLO

The agreement between NNLO PDF sets is not automatically better than at NLO

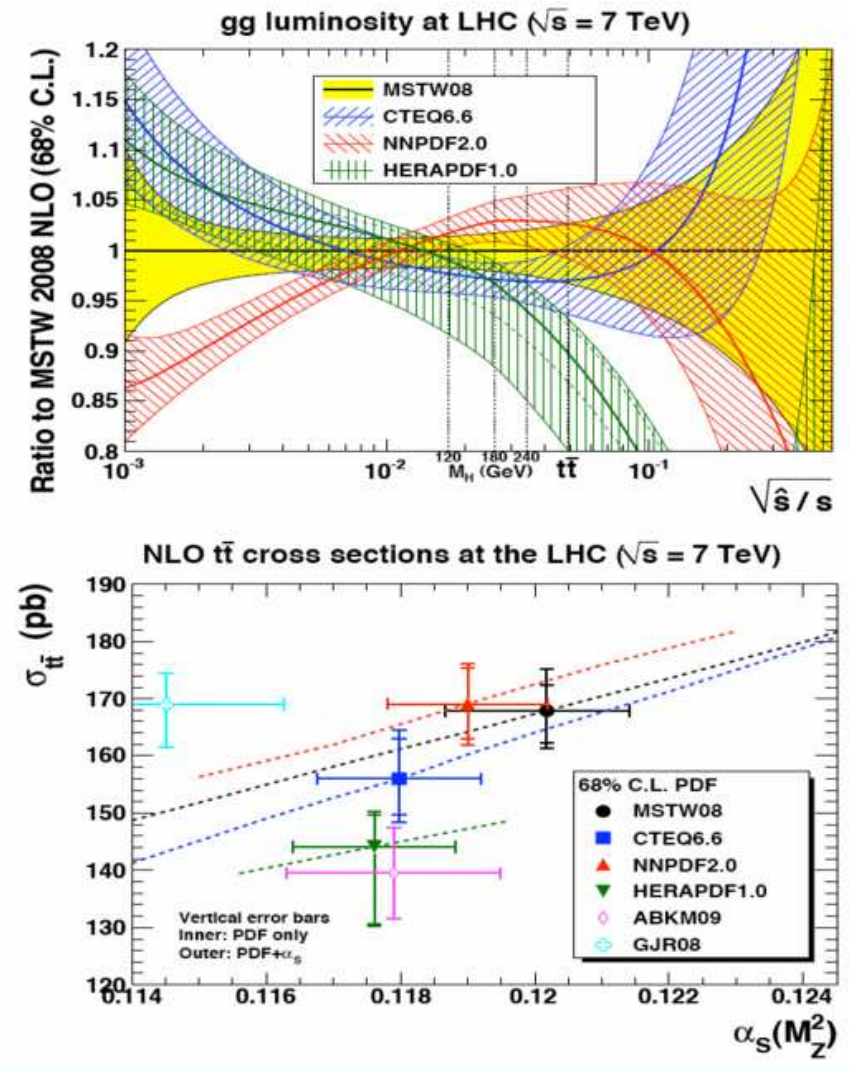

G. Watt, in PDF4LHC study, arXiv:1101.0536

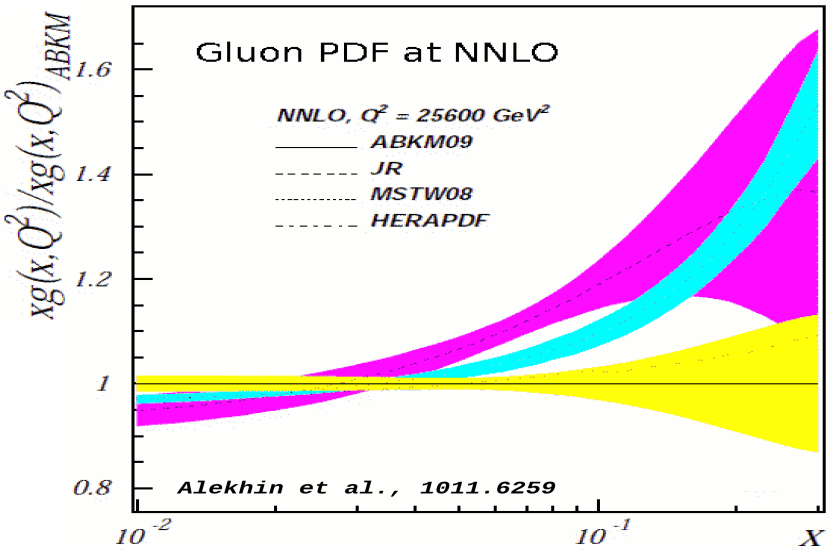

NNLO gg→H at the Tevatron (√s = 1.96 TeV) for M_H = 180 GeV

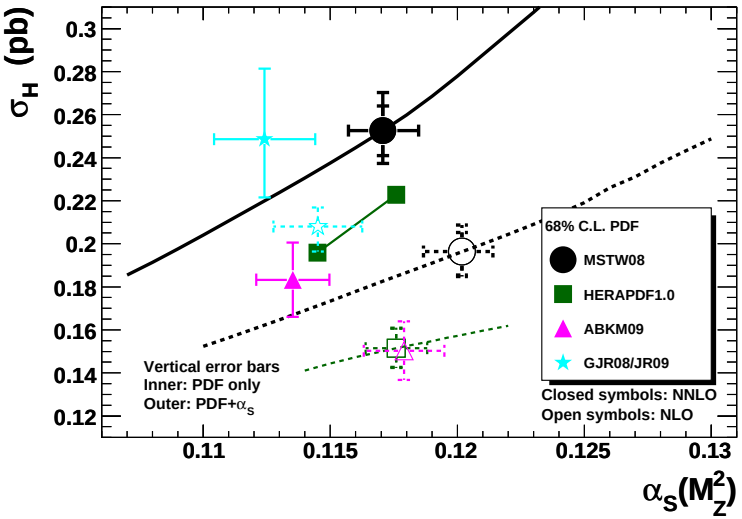

$\chi^2/N_{data\,points}$ in various experiments (PRELIMINARY)

PDF set	Order	All expts.	Combined HERA-1 DIS	BCDMS $F_2^{p,d}$	CDF, D0 Run-2 1-jet	D0 Run-2 A^e_{ch}, $p^e_T > 25$ GeV
CT10.1	NLO	**1.11**	**1.17**	**1.10**	**1.33**	**3.72**
MSTW08	NLO	1.42 (1.28)	1.73 (1.4)	1.16 (1.17)	1.31	11.38
NNPDF2.0	NLO	1.37	1.32	1.28	1.57	**2.79**
CT10.1	NNLO	**1.13**	**1.12**	**1.14**	**1.23**	**2.59**
MSTW08	NNLO	1.34	1.36	**1.15**	1.38	9.84
NNPDF2.1	NNLO	1.57	1.36	1.30	1.51	5.45
ABM'09 (5f)	NNLO	1.65	1.4	1.49	2.63	**23.78**
HERA1.5	NNLO	1.71	**1.15**	**1.87**	**?**	5.4
N_{points}		2798	579	590	182	12

Cross sections are computed using the CTEQ fitting code and α_s, m_c, m_b values provided by each PDF set. Their agreement does not immediately improve after going to NNLO.

Origin of differences between PDF sets

- **NNLO QCD** terms *(in all 6 PDF fits)*
  - **Implementation of heavy-quark mass** terms
- **(N)LO electroweak** contributions
- **Selection of data**: global analyses *(CTEQ, MSTW, NNPDF)* vs. restricted ("DIS-based") analyses *(ABM, GJR, HERAPDF)*
- **Statistical treatment**: Monte-Carlo sampling vs. analytical minimization of χ^2; correlated systematic uncertainties; definitions of PDF uncertainties
- **Initial PDF parametrizations**: neural networks *(NNPDF)*; 2-5 parameters per flavor *(other fits)*
- **Values of** $\alpha_s(M_Z)$, m_c, **and** m_b and their treatment
- **Differences in NLO codes** used by PDF fits

This talk

Genuine NNLO accuracy requires an earnest effort to calibrate all components of the PDF fits

I will provide examples of related activities, focusing on

- Heavy-quark contributions to DIS at $\mathcal{O}(\alpha_s^2)$

  M. Guzzi, P.N., H.-L. Lai, C.-P. Yuan, ***arXiv:1108.5112****;*

  additional figures at ***http://bit.ly/SACOTNNLO11***

- W charge asymmetry at the Tevatron

  1. H.-L. Lai, M. Guzzi, J. Huston, Z. Li, P. N., J. Pumplin, C.-P. Yuan, Phys.Rev. D82 (2010) 074024.

  2. M. Guzzi, P. N., E. Berger, H.-L. Lai, F. Olness, C.-P. Yuan, arXiv:1101.0561 (hep-ph).

- Consistency of DGLAP picture at small x at HERA

  1. H.-L. Lai, M. Guzzi, J. Huston, Z. Li, P. N., J. Pumplin, C.-P. Yuan, Phys.Rev. D82 (2010) 074024.

1. Heavy quarks in DIS and LHC electroweak cross sections

The latest PDF fits assume $m_{c,b} \neq 0$ when evaluating Wilson coefficients in DIS, $e^{\pm}p \to e^{\pm}X$ and $e^{\pm}p \to \nu X$

This is needed, in particular, to correctly predict W, Z production rates at the LHC *(Tung et al., hep-ph/0611254)*

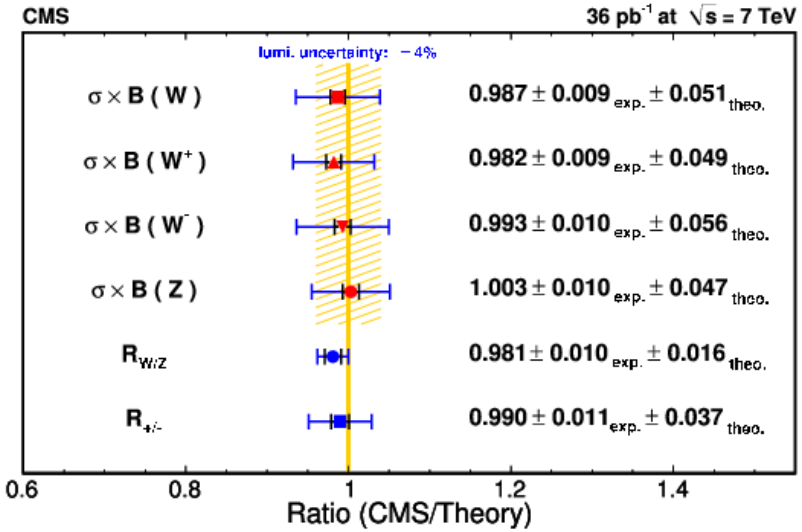

CMS-PAS-EWK-10-005

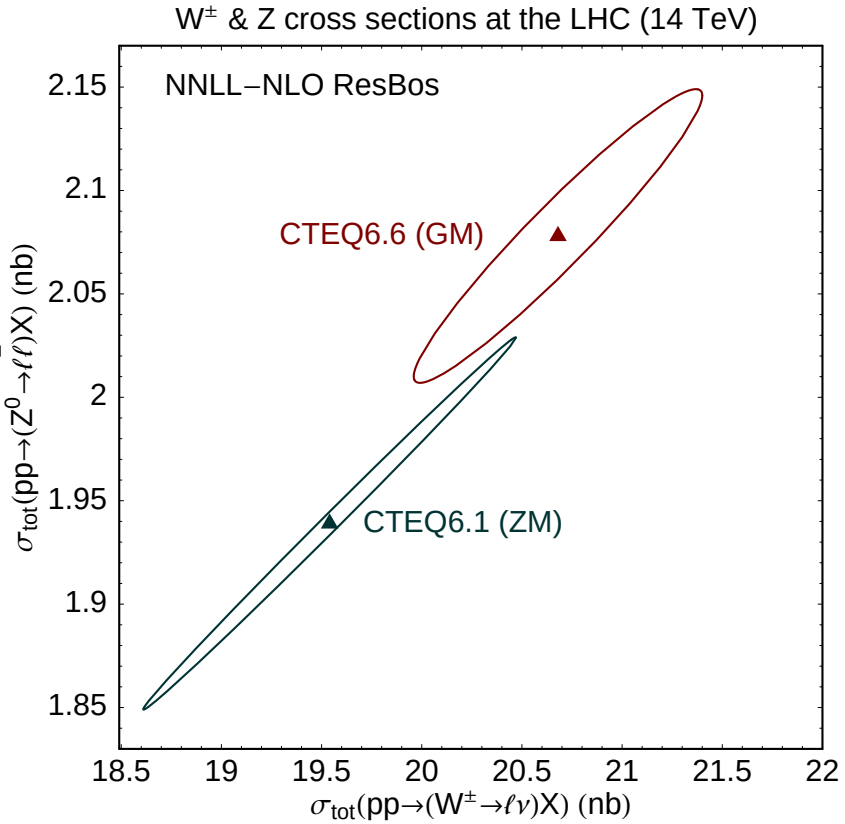

arXiv:0802.0007

1. Heavy quarks in DIS and LHC electroweak cross sections

In $pp \to Z^0 X$ at $\sqrt{s} = 14$ TeV:

$$\frac{\sigma(\text{general-mass PDFs})}{\sigma(\text{zero-mass PDFs})} \approx 1.05 - 1.08;$$

to be compared with

$$K_{NNLO/NLO} \equiv \sigma(\alpha_s^2)/\sigma(\alpha_s) \approx 1.02$$

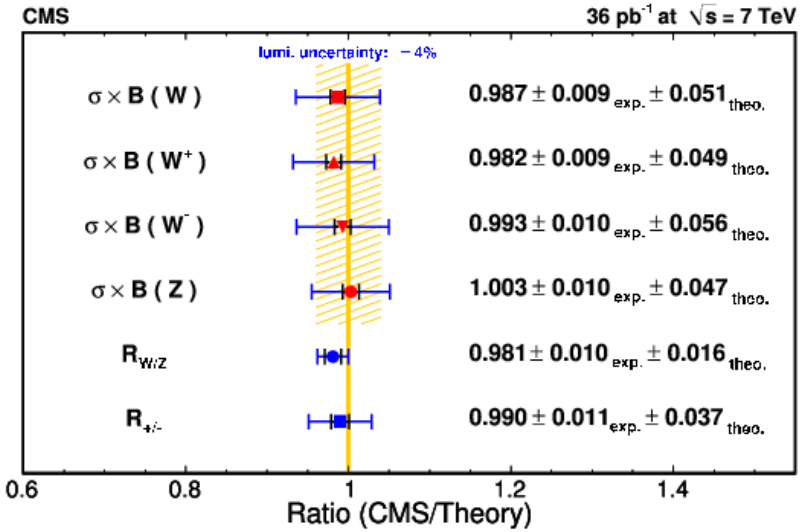

CMS-PAS-EWK-10-005

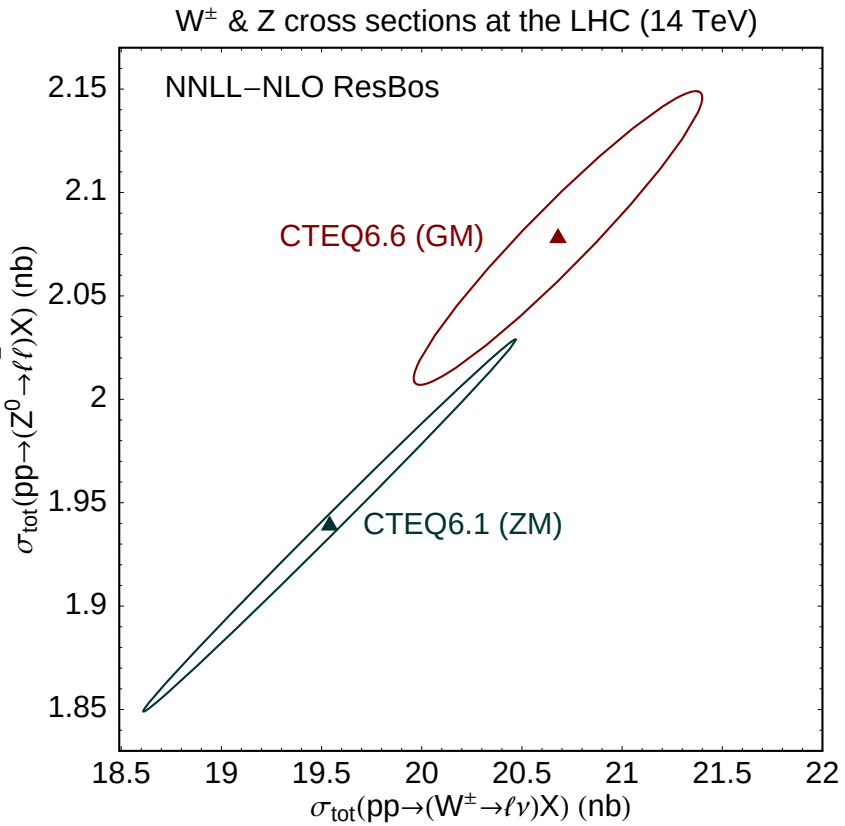

arXiv:0802.0007

Massive quark contributions to neutral-current DIS

Several heavy-quark factorization schemes

FFN, ACOT, BMSN, CSN, FONLL, TR'...

Extensive recent work

Tung et al., hep-ph/0611254; Thorne, hep-ph/0601245; Tung, Thorne, arXiv:0809.0714; P.N., Tung, arXiv:0903.2667; Forte, Laenen, Nason, arXiv:1001.2312; J. Rojo et al., arXiv:1003.1241;Alekhin, Moch, arXiv:1011.5790;...

Is a consistent picture emerging? Will persisting confusions (e.g., about the universality of heavy-quark PDFs) be resolved?

Heavy-quark NC DIS at NLO: consistent ambiguity

At NLO, the charm mass m_c and factorization scale μ of are **tuned** to best describe the DIS data in each scheme; but the residual differences in the W and Z cross sections remain

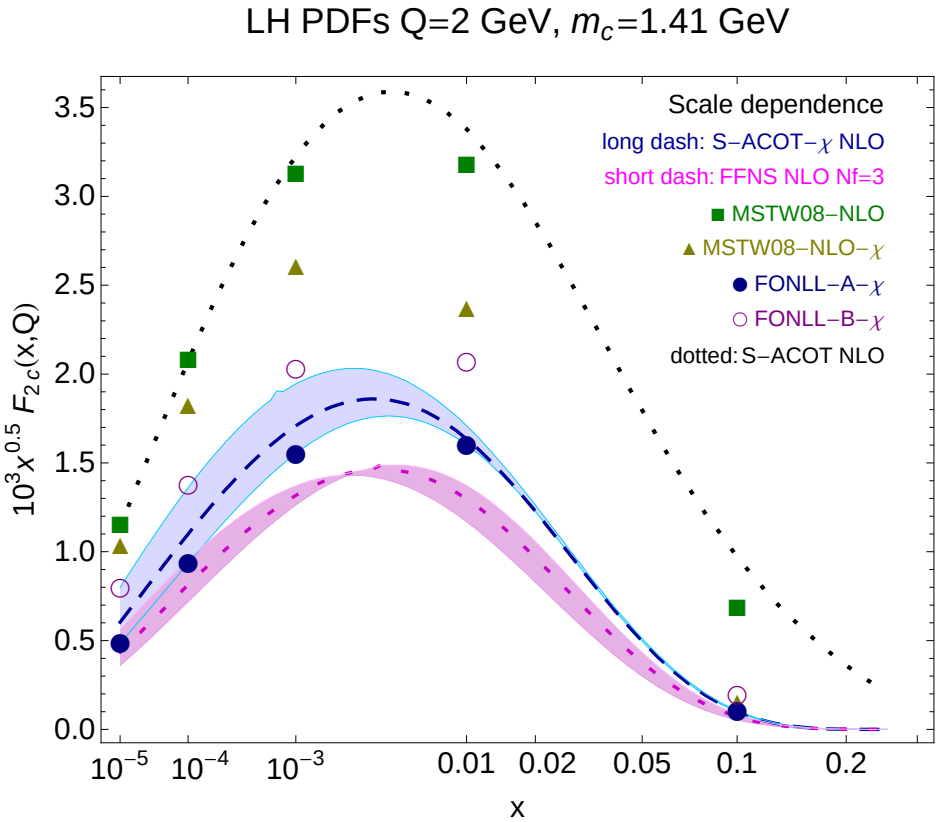

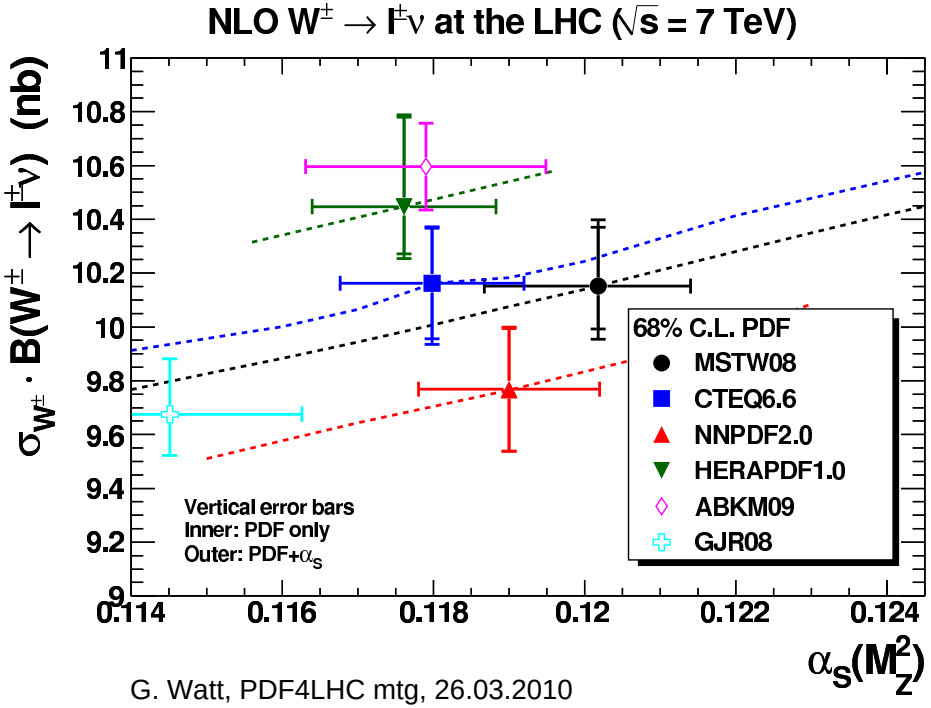

G. Watt, PDF4LHC mtg, 26.03.2010

2009 Les Houches HQ benchmarks with toy PDFs; default $\mu = Q$

W, Z cross sections; $m_c = 1.3$ GeV in CTEQ6.6

NNLO: better agreement between the schemes, remaining conceptual differences

arXiv:1108.5112

- revisits the QCD factorization theorem for DIS with heavy quarks
- discusses a scheme (S-ACOT-χ) for a streamlined, algorithmic implementation of NNLO massive contributions

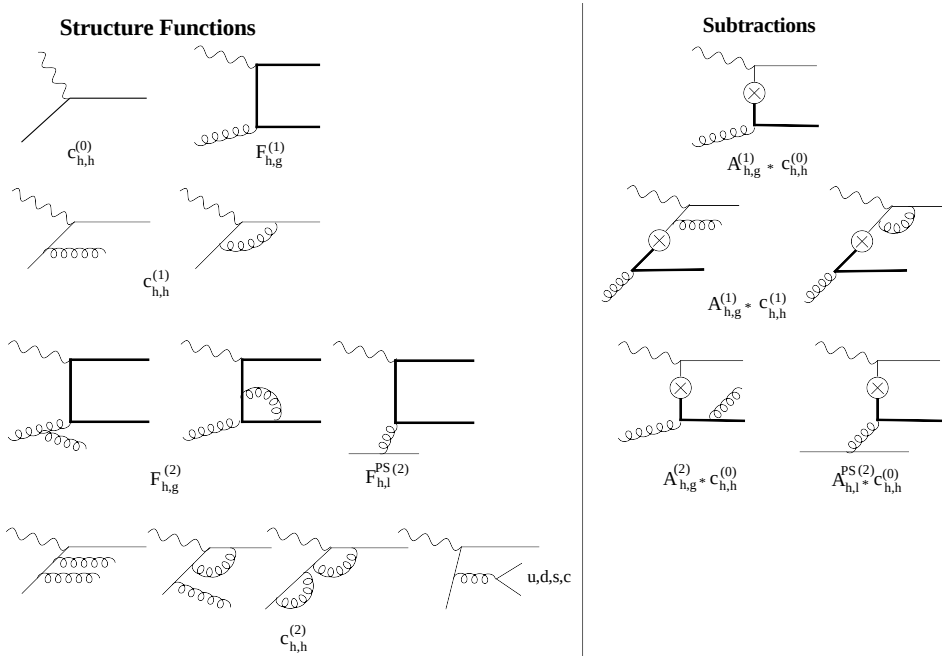

S-ACOT-χ scheme: merging FFN and ZM

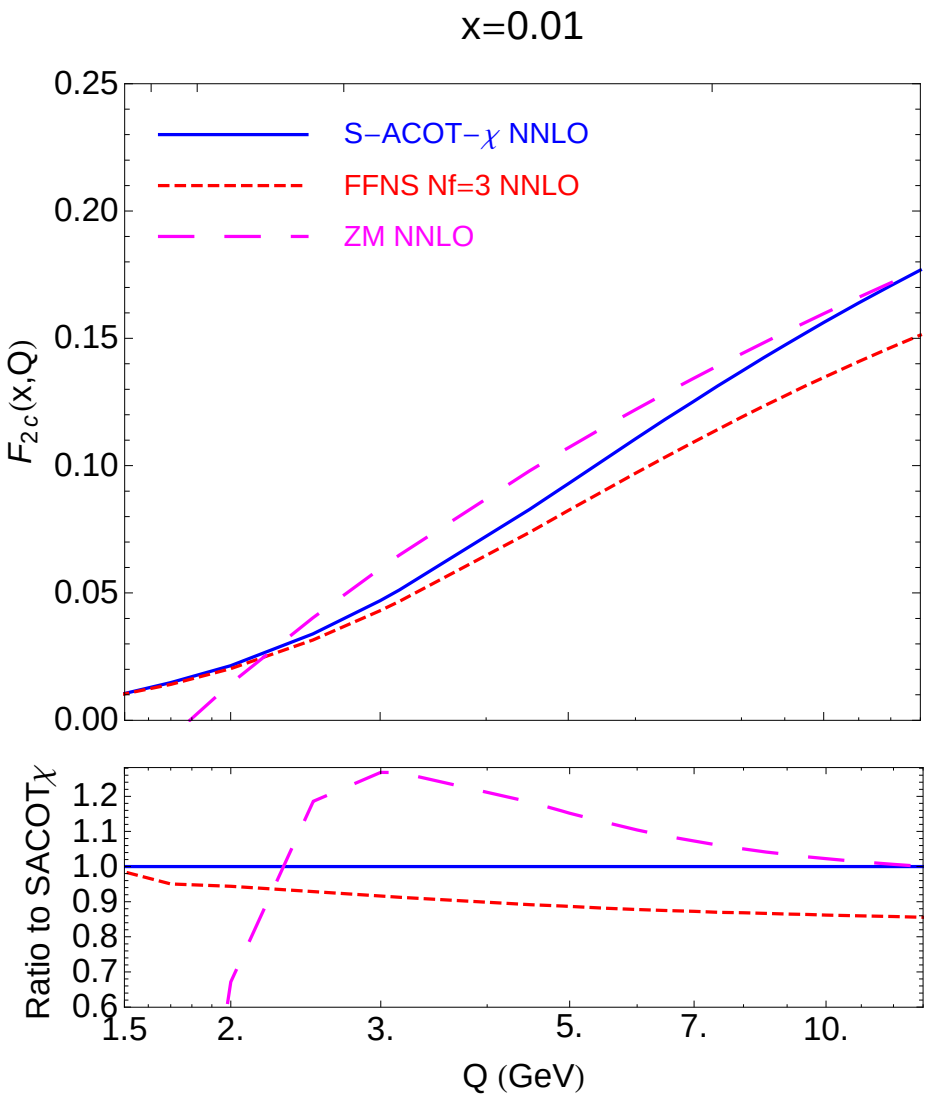

S-ACOT-χ reduces to FFN at $Q \approx m_c$ and to ZM at $Q \gg m_c$

Les Houches toy PDFs, evolved at NNLO with threshold matching terms

Cancellations between subtractions and other terms at $Q \approx m_c$ and $Q \gg m_c$; details in backup slides

Are heavy quarks counted as active partons?

Fixed Flavor Number scheme

$m_c \neq 0$ for all $\mu^2 = Q^2 \geq m_c^2$

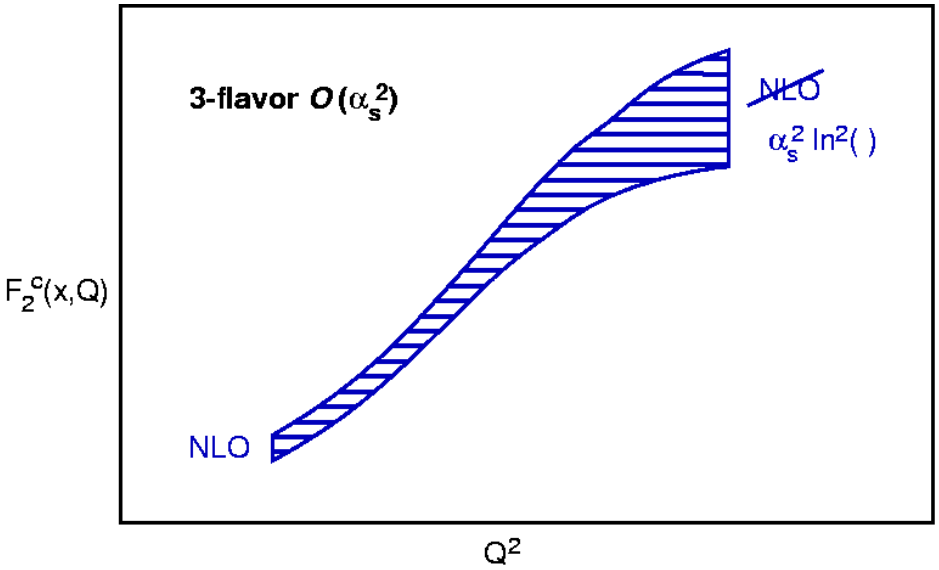

Zero-Mass Variable Flavor Number scheme

$m_c = 0$ for all $Q^2 \geq m_c^2$

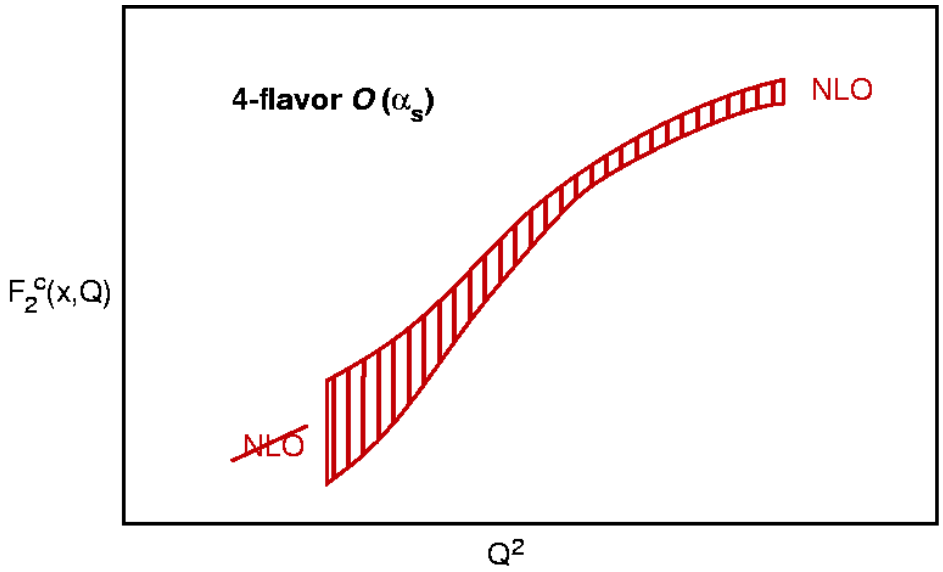

$$f_{c/p}(\xi,\mu^2) \sim \sum_{n=1}^{\infty} \alpha_S^k(\mu) \sum_{k=0}^{n} c_{nk}(\xi)\ \ln^k\left(\frac{\mu^2}{m_c^2}\right)$$

Shown for up to 4 flavors for simplicity

General-Mass Variable Flavor Number schemes

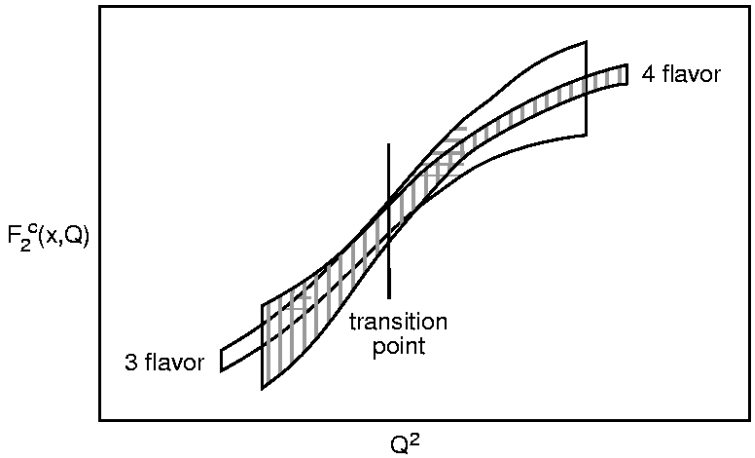

(Aivasis, Collins, Olness, Tung; Buza et al.; Cacciari, Greco, Nason; Chuvakin et al.; Kniehl et al.; Thorne, Roberts; Forte, Laenen, Nason; ...)

For the ACOT GM scheme, factorization of DIS cross sections is proved to all orders of α_s *(Collins, 1998)*

Theorem

$$F_2(x,Q,m_c) = \sigma_0 \sum_{a=g,q,\bar{q}} \int \frac{d\xi}{\xi} C_a\left(\frac{x}{\xi}, \frac{Q}{\mu_F}, \frac{m_c}{Q}\right) f_{a/p}(\xi, \frac{\mu_F}{m_c}) + \mathcal{O}\left(\frac{\Lambda_{QCD}}{Q}\right)$$

- C_a *is a Wilson coefficient with an incoming parton* $a = g, \overset{(-)}{u}, ..., \overset{(-)}{c}$
- $f_{a/p}$ *is a PDF for* N_f *flavors*
- $N_f = 3$ *for* $\mu < \mu^{(4)}_{switch} \approx m_c$; $N_f = 4$ *for* $\mu \geq \mu^{(4)}_{switch}$
- $\lim_{Q\to\infty} C_a$ *exists; no terms* $\mathcal{O}(m_c/Q)$ *in the remainder*

General-Mass Variable Flavor Number schemes

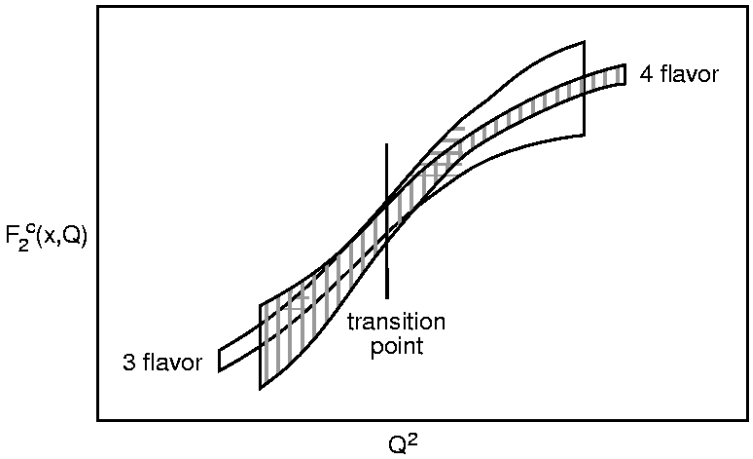

(Aivasis, Collins, Olness, Tung; Buza et al.; Cacciari, Greco, Nason; Chuvakin et al.; Kniehl et al.; Thorne, Roberts; Forte, Laenen, Nason; ...)

For the ACOT GM scheme, factorization of DIS cross sections is proved to all orders of α_s *(Collins, 1998)*

Schemes of the ACOT type do not use...

- PDFs for several N_f values in the same μ range
- smoothness conditions/damping factors at $Q \to m_c$
- constant terms from higher orders in α_s to ensure continuity at the threshold

Components of inclusive $F_{2,L}(x,Q)$

Structure of S-ACOT-χ NNLO expressions is reminiscent of the ZM scheme (e.g., in Moch, Vermaseren, Vogt, 2005)

Components of inclusive $F_{2,L}(x,Q^2)$ are classified according to the quark couplings to the photon

$$F = \sum_{l=1}^{N_l} F_l + F_h \tag{1}$$

$$F_l = e_l^2 \sum_a \left[C_{l,a} \otimes f_{a/p}\right](x,Q), \quad F_h = e_h^2 \sum_a \left[C_{h,a} \otimes f_{a/p}\right](x,Q). \tag{2}$$

At $\mathcal{O}(\alpha_s^2)$:

$$F_h^{(2)} = e_h^2 \left\{c_{h,h}^{NS,(2)} \otimes (f_{h/p} + f_{\bar{h}/p}) + C_{h,l}^{(2)} \otimes \Sigma + C_{h,g}^{(2)} \otimes f_{g/p}\right\}$$

$$F_l^{(2)} = e_l^2 \left\{C_{l,l}^{NS,(2)} \otimes (f_{l/p} + f_{\bar{l}/p}) + c^{PS,(2)} \otimes \Sigma + c_{l,g}^{(2)} \otimes f_{g/p}\right\}. \tag{3}$$

Components of inclusive $F_{2,L}(x,Q)$

- Lower case $c^{(2)}_{a,b}$, $\hat{f}^{(k)}_{a,b} \to$ ZM expressions
  Zijlstra and Van Neerven PLB272 (1991), NPB383 (1992)
  S. Moch, J.A.M. Vermaseren and A. Vogt, NPB724 (2005)

- Upper case $C^{(2)}_{a,b}$, $F^{(k)}_{a,b}$ $A^{(k)}_{a,b} \to$ coeff. functions, structure functions and subtractions with $m_c \neq 0$,
  Buza *et al.*, NPB 472 (1996); EPJC1 (1998);
  Riemersma, *et al.* PLB 347 (1995); Laenen *et al.* NPB392 (1993)

- All building blocks are available from literature

Components of inclusive $F_{2,L}(x,Q)$

The separation into F_l and F_h (according to the quark's electric charge e_i^2) is valid at all Q

The "light-quark" F_l contains some subgraphs with heavy-quark lines, denoted by "$G_{l,l,heavy}$".

The "heavy-quark" $F_h \neq F_2^c$:

$$F_2^c = F_h + (G_{l,l,heavy})_{real},$$

where $G_{i,j} = C_{i,j}^{(2)}$, $F_{i,j}^{(2)}$, and $A_{i,j}^{(2)}$

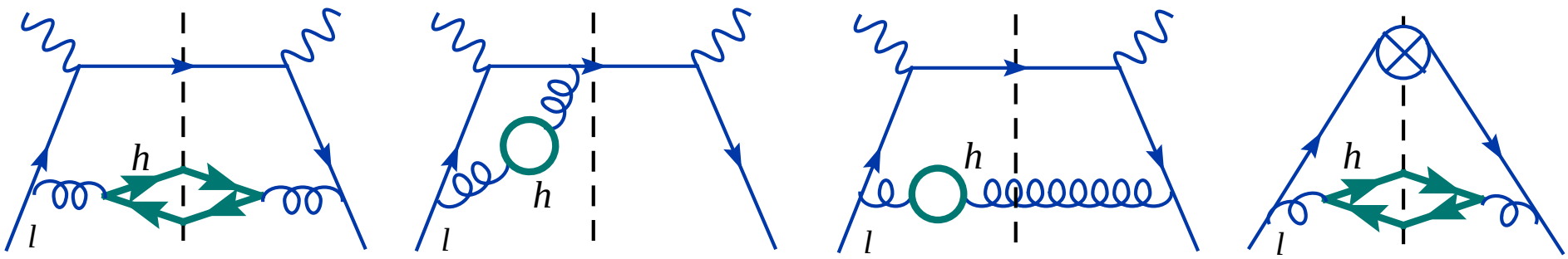

Three versions of the ACOT scheme

Scheme	Lowest-order graphs	Variables in H_c
Full ACOT *Aivasis et. al., hep-ph/9312319* *Proof in Collins, hep-ph/9806259*	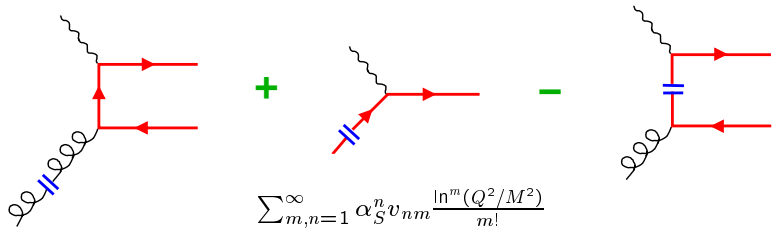	$m_c \neq 0$ $\zeta = \frac{x}{2}\left(1+\sqrt{1+\frac{4m_c^2}{Q^2}}\right)$
Simplified ACOT *Proof in Collins, hep-ph/9806259;* *Kramer, Olness, Soper, hep-ph/0003035*	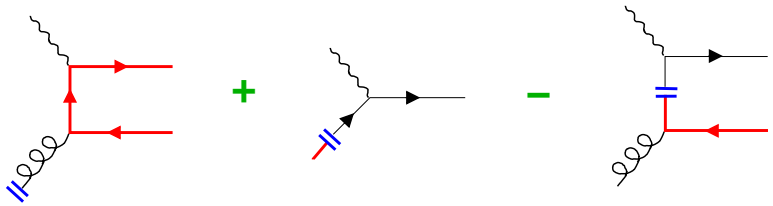	$m_c = 0$ $\zeta = x$
S-ACOT-χ *Tung, Kretzer, Schmidt, hep-ph/0110247;* *proof in Guzzi et al., arXiv:1108.5112*	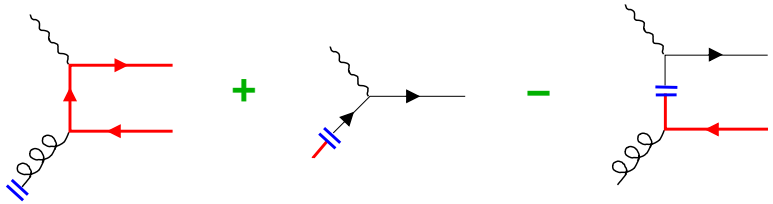	$m_c = 0$ $\zeta = x\left(1+\frac{4m_c^2}{Q^2}\right) \equiv \chi$

- H_a with incoming light partons are unambiguous

The NLO analytic result

Which would you prefer to calculate?

ACOT

$$
\begin{aligned}
\hat{f}_1^Q(\hat{s}_1) &= \frac{8}{\Delta'^2}\Big\{ -\Delta^2(S_+\Sigma_{++} - 2m_1m_2S_-)I_{\xi'} + 2m_1m_2S_-\Big(\frac{1}{\hat{s}_1}[\Delta'^2 + 4m_2^2\Sigma_{+-}] \\
&+ 2\Sigma_{+-} - \Sigma_{-+} + \frac{\Sigma_{++}+\hat{s}_1}{2} + \frac{\hat{s}_1+m_2^2}{\Delta'\hat{s}_1}\left[\Delta'^2 + 2\Sigma_{+-}\Sigma_{++} + \left(m_2^2+Q^2\right)\hat{s}_1\right]\ L_{\xi'}\Big) \\
&+ S_+\Big(\frac{-m_2^2\Sigma_{++}}{(\hat{s}_1+m_2^2)\hat{s}_1}(\Delta^2 + 4m_2^2\Sigma_{+-}) - \frac{1}{4(\hat{s}_1+m_2^2)}\Big[3\Sigma_{++}^2\Sigma_{-+} + 4m_2^2(10\Sigma_{++}\Sigma_{+-} \\
&- \Sigma_{+-}\Sigma_{-+} - m_1^2\Sigma_{++}) + \hat{s}_1[-7\Sigma_{++}\Sigma_{-+} + 18\Delta^2 - 4m_1^2(7Q^2 - 4m_2^2 + 7m_1^2)] \\
&+ 3\hat{s}_1^2[\Sigma_{+-} - 2m_1^2] - \hat{s}_1^3\Big] + \frac{\hat{s}_1+m_2^2}{2\Delta'}\Big[\frac{-2}{\hat{s}_1}\Sigma_{++}\left(\Delta^2 + 2\Sigma_{+-}\Sigma_{++}\right) \\
&+ \left(4m_1^2m_2^2 - 7\Sigma_{+-}\Sigma_{++}\right) - 4\Sigma_{+-}\hat{s}_1 - \hat{s}_1^2\Big]\ L_{\xi'}\Big)\Big\} \\
\hat{f}_2^Q(\hat{s}_1) &= \frac{16}{\Delta'^4}\Big\{ -2\Delta^4 S_+ I_{\xi'} + 2m_1m_2S_-\Big(\frac{\hat{s}_1+m_2^2}{\Delta'}\left(\Delta'^2 - 6m_1^2Q^2\right)\ L_{\xi'} \\
&- \frac{\Delta'^2(\hat{s}_1+\Sigma_{++})}{2(\hat{s}_1+m_2^2)} + \left(2\Delta'^2 - 3Q^2\left(\hat{s}_1+\Sigma_{++}\right)\right)\Big) + S_+\Big(-2(\Delta^2 - 6m_1^1Q^2)(\hat{s}_1+m_2^2) \\
&- 2\left(m_1^2+m_2^2\right)\hat{s}_1^2 - 9m_2^2\Sigma_{+-}^2 + \Delta^2\left(2\Sigma_{++} - m_2^2\right) + 2\hat{s}_1\left(2\Delta^2 + \left(m_1^2 - 5m_2^2\right)\Sigma_{+-}\right) \\
&+ \frac{\left(\Delta'^2 - 6Q^2\left(m_2^2+\hat{s}_1\right)\right)\Sigma_{++}\left(\hat{s}_1+\Sigma_{++}\right)}{2(\hat{s}_1+m_2^2)} - \frac{2\Delta^2}{\hat{s}_1}\left(\Delta^2 + 2(2m_2^2+\hat{s}_1)\Sigma_{+-}\right) \\
&+ \frac{(\hat{s}_1+m_2^2)}{\Delta'}[\frac{-2}{\hat{s}_1}\Delta^2(\Delta^2 + 2\Sigma_{+-}\Sigma_{++}) - 2\hat{s}_1(\Delta^2 - 6m_1^2Q^2) \\
&- (\Delta'^2 - 18m_1^2Q^2)\Sigma_{++} - 2\Delta^2\left(\Sigma_{++} + 2\Sigma_{+-}\right)]\ L_{\xi'}\Big)\Big\} \\
\hat{f}_3^Q(\hat{s}_1) &= \frac{16}{\Delta'^2}\Big\{ -2\Delta^2 R_+ I_{\xi'} + 2m_1m_2R_-\left(1 - \frac{\Sigma_{-+}}{\hat{s}_1} + \frac{(\hat{s}_1+m_2^2)\left(\hat{s}_1+\Sigma_{+-}\right)}{\Delta'\hat{s}_1}\ L_{\xi'}\right) \\
&+ R_+\Big(\Sigma_{-+} - 3\Sigma_{+-} - \frac{2}{\hat{s}_1}\left(\Delta^2 + 2m_2^2\Sigma_{+-}\right) - \frac{(\hat{s}_1 - \Sigma_{-+})(\hat{s}_1+\Sigma_{++})}{2(\hat{s}_1+m_2^2)} \\
&+ \frac{\hat{s}_1+m_2^2}{\Delta'\hat{s}_1}\left[-\hat{s}_1^2 + 4\left(m_1^2\Sigma_{-+} - \Delta^2\right) - 3\hat{s}_1\Sigma_{+-}\right]\ L_{\xi'}\Big)\Big\}
\end{aligned}
$$

with

$$L_{\xi'} \equiv \ln\left(\frac{\Sigma_{++}+\hat{s}_1-\Delta'}{\Sigma_{++}+\hat{s}_1+\Delta'}\right)$$

and

$$I_{\xi'} = \left(\frac{\hat{s}_1+2m_2^2}{\hat{s}_1^2} + \frac{\hat{s}_1+m_2^2}{\Delta'\hat{s}_1^2}\Sigma_{++}\ L_{\xi'}\right) .$$

F. Olness, 2002

S-ACOT

$$
\begin{aligned}
C_2^{(Vq)(1)} &= C_2(F)\frac{x}{2}\left[\frac{1+x^2}{1-x}\left(\ln\frac{(1-x)}{x} - \frac{3}{4}\right) + \frac{1}{4}(9+5x)\right]_+ , \\
C_1^{(Vq)(1)} &= \frac{1}{2x}C_2^{(Vq)(1)} - C_2(F)\frac{1}{2}x , \\
C_3^{(Vq)(1)} &= \frac{1}{x}C_2^{(Vq)(1)} - C_2(F)(1+x) ,
\end{aligned}
$$

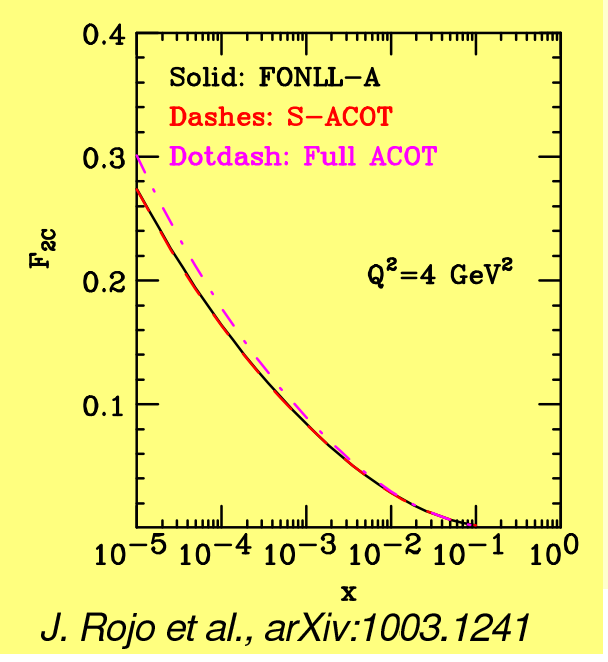

J. Rojo et al., arXiv:1003.1241

Three versions of the ACOT scheme

Scheme	Lowest-order graphs	Variables in H_c
Full ACOT *Aivasis et. al., hep-ph/9312319* *Proof in Collins, hep-ph/9806259*	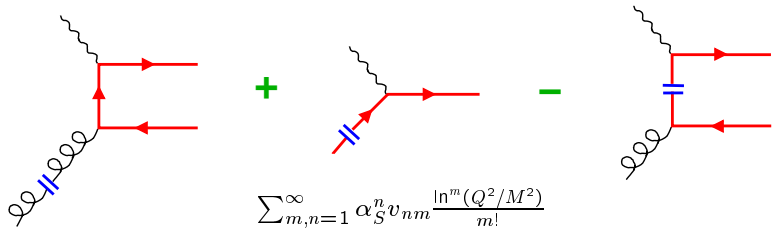	$m_c \neq 0$ $\zeta = \frac{x}{2}\left(1+\sqrt{1+\frac{4m_c^2}{Q^2}}\right)$
Simplified ACOT *Proof in Collins, hep-ph/9806259;* *Kramer, Olness, Soper, hep-ph/0003035*	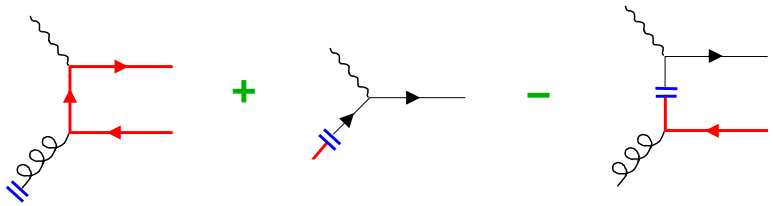	$m_c = 0$ $\zeta = x$
S-ACOT-χ *Tung, Kretzer, Schmidt, hep-ph/0110247;* *proof in Guzzi et al., arXiv:1108.5112*	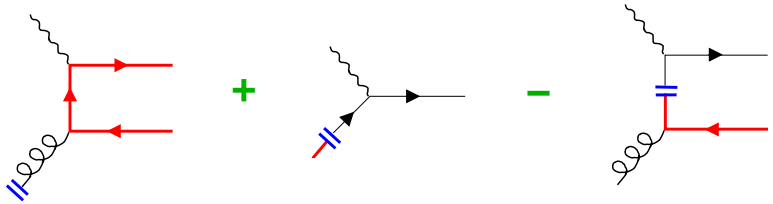	$m_c = 0$ $\zeta = x\left(1+\frac{4m_c^2}{Q^2}\right) \equiv \chi$

- H_a with incoming light partons are unambiguous

Energy conservation near the threshold

Threshold rate suppression resulting from energy conservation is the most important mass effect at $Q \approx m_c$

(Tung, Kretzer, Schmidt, hep-ph/0110247; Tung, Thorne, arXiv:0809.0714; P.N., Tung, arXiv:0903.2667)

In DIS, a $c\bar{c}$ pair is produced only at partonic energies $\widehat{W}$ satisfying

$$\widehat{W}^2 = (\xi p + q)^2 = Q^2 \left(\frac{\xi}{x} - 1 \right) \geq 4m_c^2$$

$$\Rightarrow \chi \leq \xi \leq 1, \text{ where } \chi \equiv x \left(1 + \frac{4m_c^2}{Q^2} \right) \geq x.$$

☹ Collinear approximation for $c\bar{c}$ production may allow to integrate over

$$x \leq \xi \leq 1,$$

in violation of energy conservation

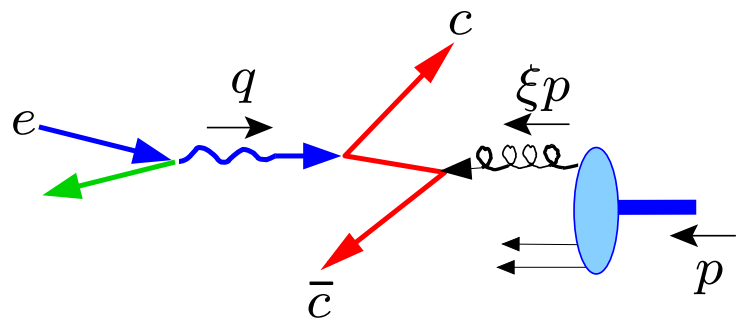

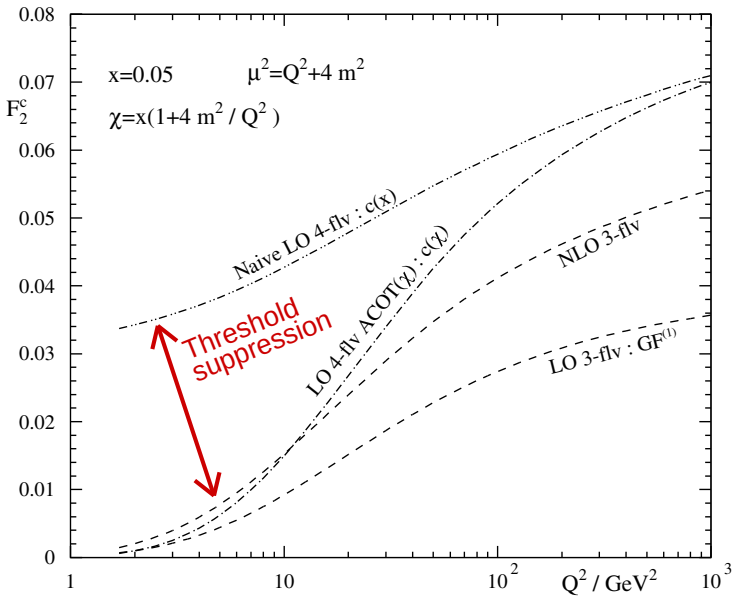

Energy conservation near the threshold

Threshold rate suppression resulting from energy conservation is the most important mass effect at $Q \approx m_c$

(Tung, Kretzer, Schmidt, hep-ph/0110247; Tung, Thorne, arXiv:0809.0714; P.N., Tung, arXiv:0903.2667)

☺ The S-ACOT-χ scheme allows one to include the energy conservation requirement in the **QCD factorization theorem** *(arXiv:1108.5112)*

☺ This is achieved by *rescaling*, which restores the correct kinematics of HQ production at the threshold without *a posteriori* constraints or damping factors imposed by other schemes

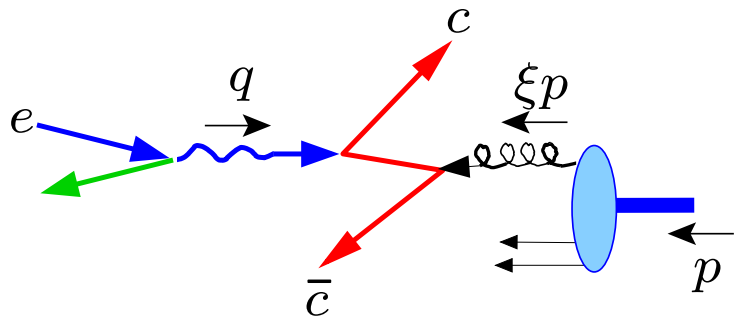

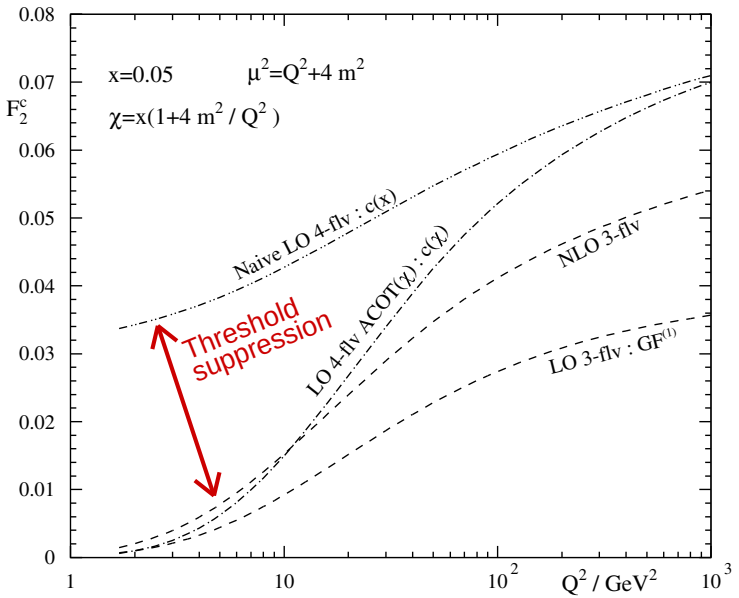

Rescaling at the lowest order

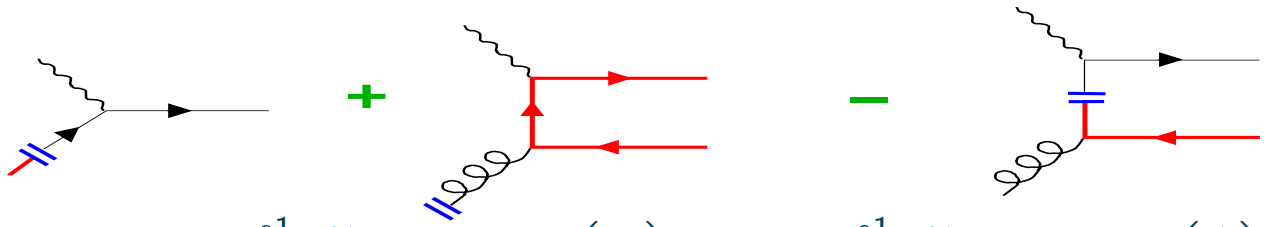

$$c(\zeta) + \frac{\alpha_s}{4\pi}\int_\chi^1 \frac{d\xi}{\xi} g(\xi) C_{h,g}^{(1)}\left(\frac{\chi}{\xi}\right) - \frac{\alpha_s}{4\pi}\int_\zeta^1 \frac{d\xi}{\xi} g(\xi) A_{h,g}^{(1)}\left(\frac{\zeta}{\xi}\right)$$

ζ takes place of x in terms 1 and 3

- Term 2 ($\gamma^* g$ fusion) is unambiguous
- Terms 1 and 3 are essentially

$$\int_0^1 \frac{d\xi}{\xi}\delta\left(1-\frac{\zeta}{\xi}\right) c(\xi) - \frac{\alpha_s}{4\pi}\int_0^1 \frac{d\xi}{\xi} g(\xi) A_{h,g}^{(1)}\left(\frac{\zeta}{\xi}\right)\theta\left(1-\frac{\zeta}{\xi}\right).$$

Rescaling $\zeta \to \kappa\zeta$, $\xi \to \kappa^{-1}\xi$ changes the ξ range in the **Wilson** coefficients $\delta(1-\frac{\zeta}{\xi})$ and $A_{h,g}^{(1)}\left(\frac{\zeta}{\xi}\right)\theta\left(1-\frac{\zeta}{\xi}\right)$, but does not change their magnitude

Rescaling at the lowest order

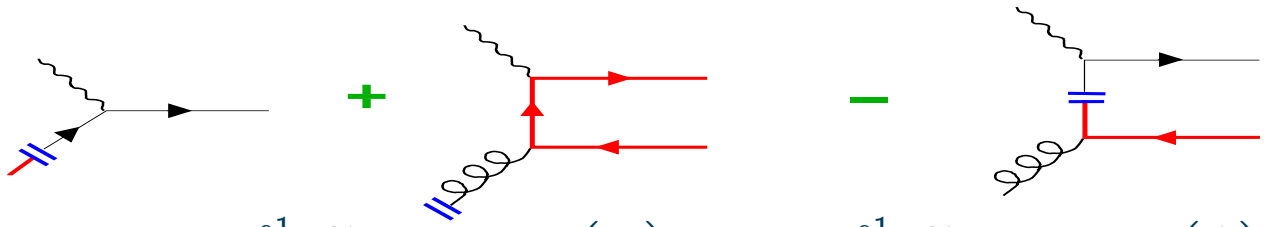

$$c(\zeta) + \frac{\alpha_s}{4\pi}\int_\chi^1 \frac{d\xi}{\xi} g(\xi) C_{h,g}^{(1)}\left(\frac{\chi}{\xi}\right) - \frac{\alpha_s}{4\pi}\int_\zeta^1 \frac{d\xi}{\xi} g(\xi) A_{h,g}^{(1)}\left(\frac{\zeta}{\xi}\right)$$

ζ takes place of x in terms 1 and 3

$Q^2 = 10$ GeV^2

- Red curve: $g(\xi)C_{h,g}^{(1)}(\chi/\xi)$ at $\chi \le \xi \le 1$
- Green: $\zeta = \mathbf{x}$; $\kappa = 1$
  - $g(\xi)A_{h,g}^{(1)}(x/\xi) \neq 0$ at $\xi < \chi$
  - its integral cancels poorly with $c(x)$
- Blue: $\zeta = \chi$; $\kappa = 1 + 4m_c^2/Q^2$
  - $g(\xi)A_{h,g}^{(1)}(\chi/\xi) = 0$ at $\xi < \chi$
  - its integral cancels better with $c(\chi)$

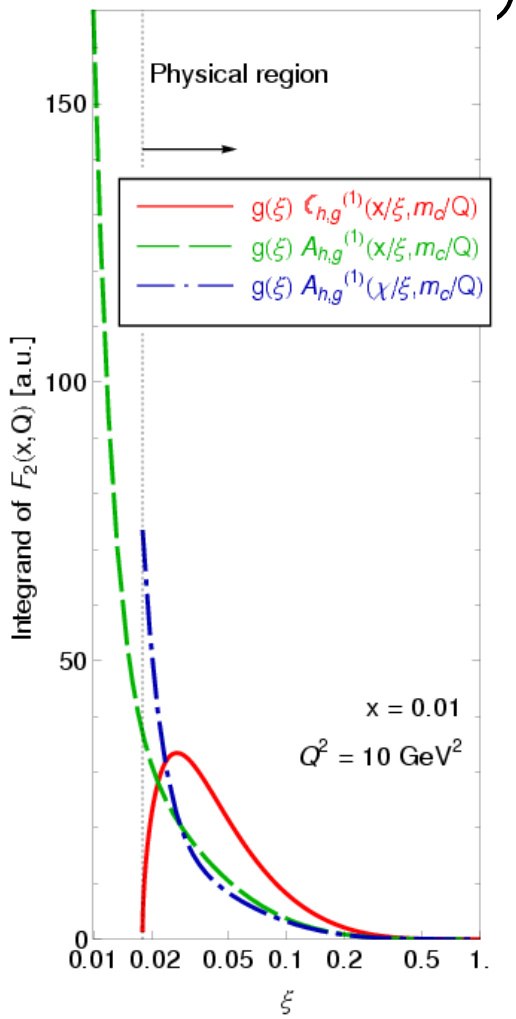

Rescaling at the lowest order

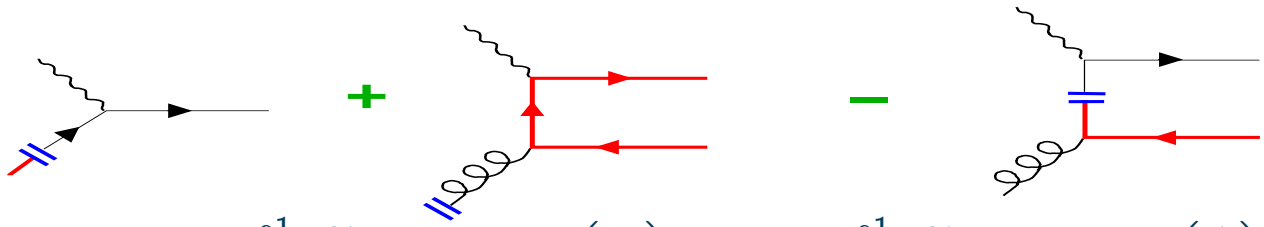

$$c(\zeta) + \frac{\alpha_s}{4\pi}\int_\chi^1 \frac{d\xi}{\xi} g(\xi) C^{(1)}_{h,g}\left(\frac{\chi}{\xi}\right) - \frac{\alpha_s}{4\pi}\int_\zeta^1 \frac{d\xi}{\xi} g(\xi) A^{(1)}_{h,g}\left(\frac{\zeta}{\xi}\right)$$

ζ takes place of x in terms 1 and 3

$Q^2 = 100$ **GeV**^{2}

$\chi \approx x$

$g(\xi)A^{(1)}_{h,g}(\zeta/\xi)$ approximates the logarithmic growth in $g(\xi)C^{(1)}_{h,g}(\chi/\xi)$

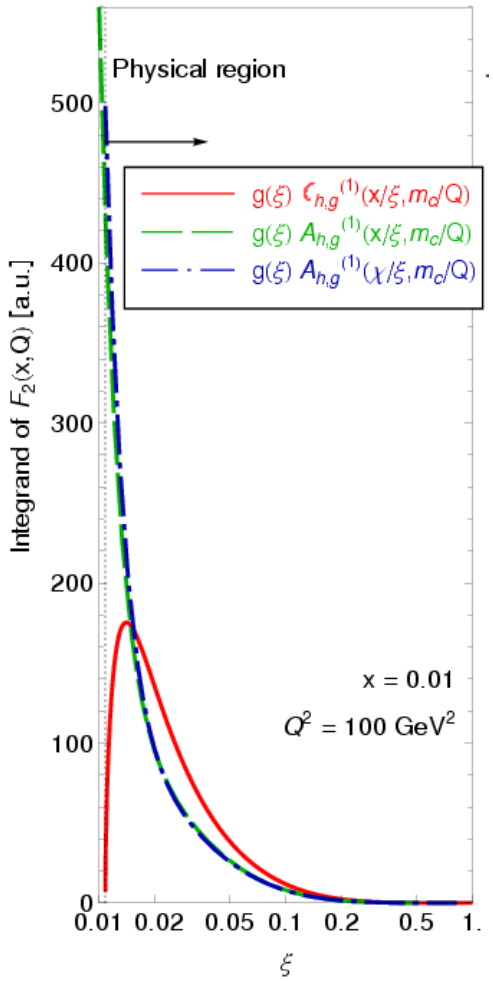

Rescaling at the lowest order

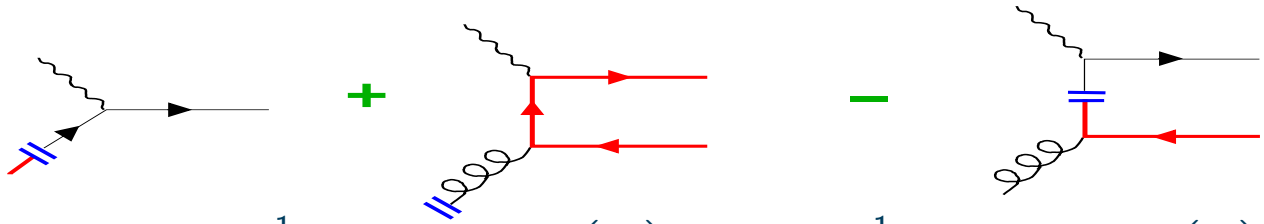

$$c(\zeta) + \frac{\alpha_s}{4\pi}\int_\chi^1 \frac{d\xi}{\xi} g(\xi) C_{h,g}^{(1)}\left(\frac{\chi}{\xi}\right) - \frac{\alpha_s}{4\pi}\int_\zeta^1 \frac{d\xi}{\xi} g(\xi) A_{h,g}^{(1)}\left(\frac{\zeta}{\xi}\right)$$

ζ takes place of x

$Q^2 = 10000$ **GeV**^{2}

$\chi \approx x$

$g(\xi)A_{h,g}^{(1)}(\zeta/\xi)$ approximates the logarithmic growth in $g(\xi)C_{h,g}^{(1)}(\chi/\xi)$

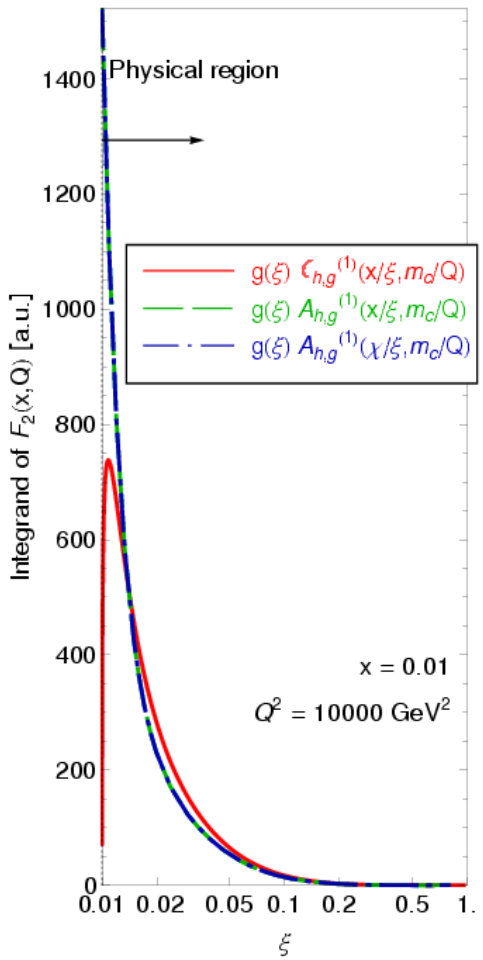

Rescaling to all orders of α_s and the factorization theorem

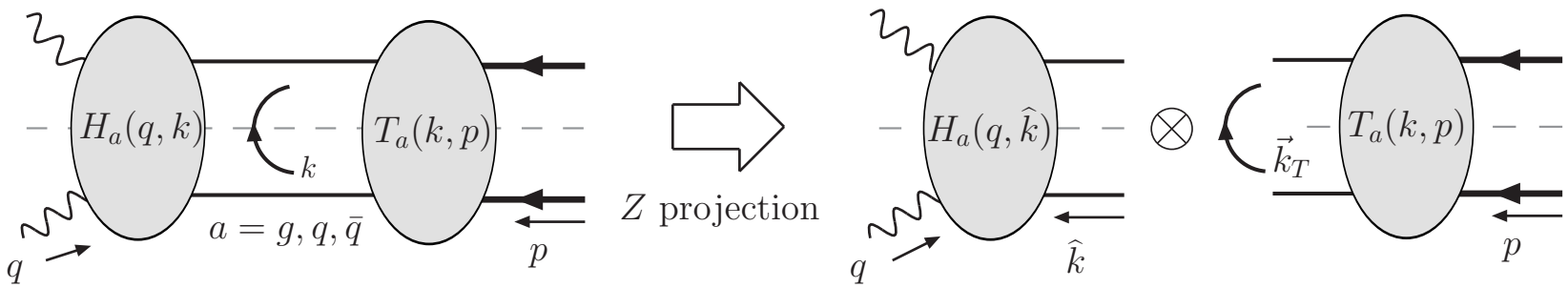

- Rescaling is introduced in the definition of the hard subgraph $H_c(q,\widehat{k})$ with an incoming c quark in $\gamma^*(q) + c(\widehat{k}) \to X$. Hard graphs $H_g,\ H_q$ with incoming light partons and target graphs $T_a(k,p)$ are not affected

- In $H_c(q,\widehat{k})$, the momentum of the incoming c quark is approximated by $\widehat{k} = \left(\xi p^+, 0^-, \vec{0}_T\right) . \widehat{k}$ and $H_c(q,\widehat{k})$ are invariant under transformation $p^+ \to p^+/\kappa$, $\xi \to \xi\,\kappa$. The physical ξ range is obtained for $\kappa = 1 + 4m_c^2/Q^2$.

- This transformation shows that the S-ACOT-χ scheme is valid to all orders on the same grounds as the S-ACOT scheme.

Rescaling to all orders of α_s and the factorization theorem

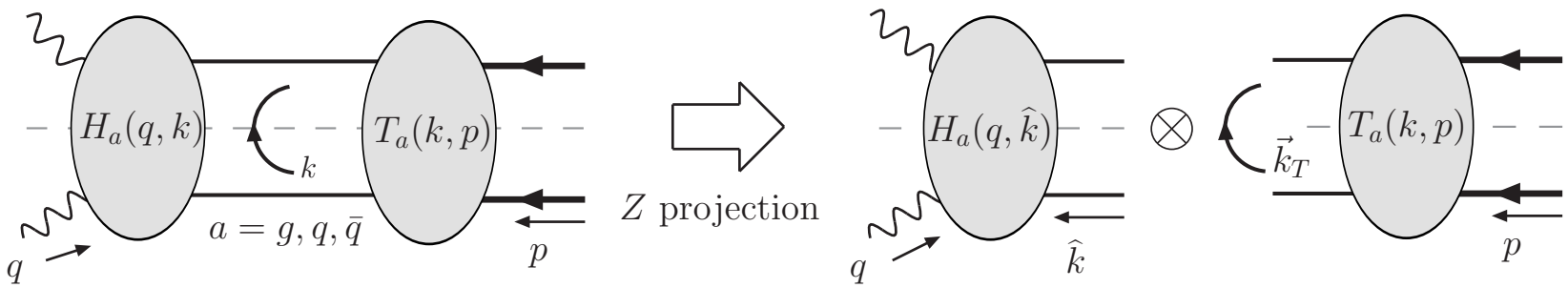

$$F(x,Q) = \sum_{a=g,u,d,\ldots,c} \int \frac{d\xi}{\xi} C_a\left(\frac{x}{\xi}, \frac{Q}{\mu}, \frac{m_c}{Q}\right) f_{a/p}(\xi,\mu)$$

- **Wilson coefficients with initial heavy quarks** are

$$C_c\left(\frac{x}{\xi}, \frac{Q}{\mu}, \frac{m_c}{Q}\right) \approx C_c\left(\frac{\chi}{\xi}, \frac{Q}{\mu}, m_c = 0\right) \theta(\chi \le \xi \le 1)$$

$$\textbf{where } \chi \equiv x\left(1 + \frac{4m_c^2}{Q^2}\right).$$

- The target (PDF) subgraphs T_a are given by the same **universal** operator matrix elements in all ACOT schemes

NNLO results for $F_2^{(c)}(x, Q^2)$

At NLO:

LH PDFs Q=2 GeV, m_c=1.41 GeV

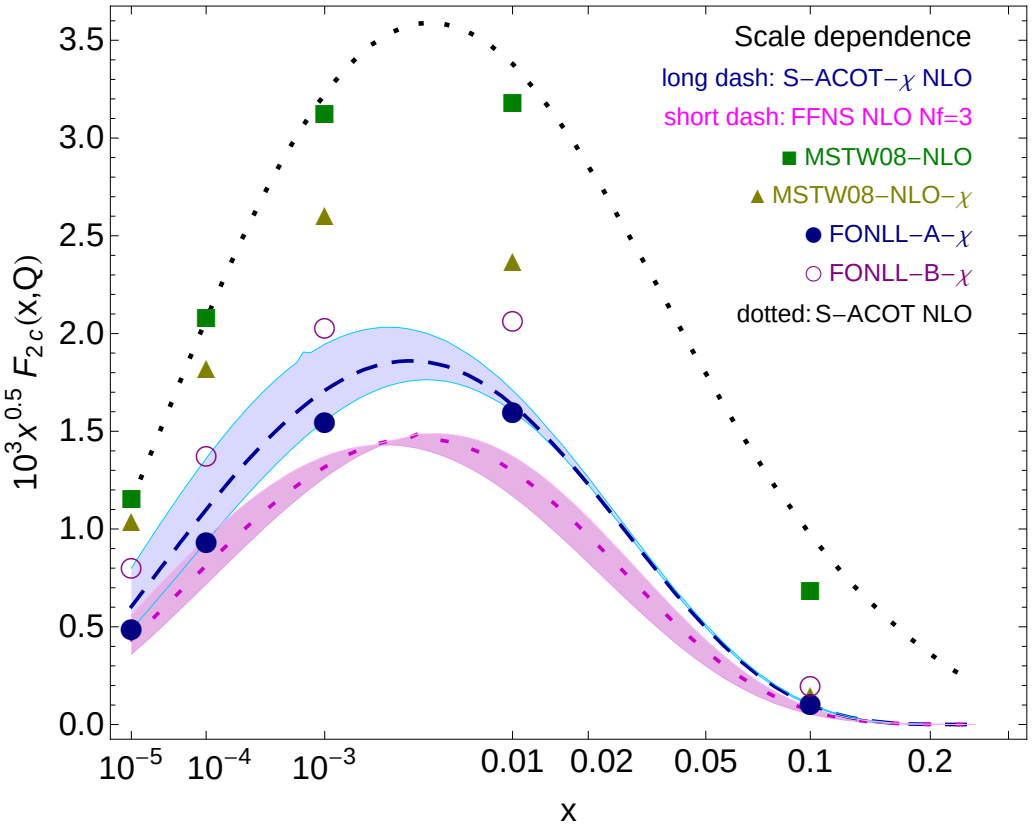

NNLO results for $F_2^{(c)}(x, Q^2)$

At NNLO and $Q \approx m_c$:

S-ACOT-χ ($N_f = 4$) $\approx$ FFN ($N_f = 3$) **without tuning**

- S-ACOT is numerically close to other NNLO schemes
- NNLO expressions are close to the FONLL-C scheme

(Forte, Laenen, Nason, arXiv:1001.2312).

LH PDFs Q=2 GeV, m_c=1.41 GeV

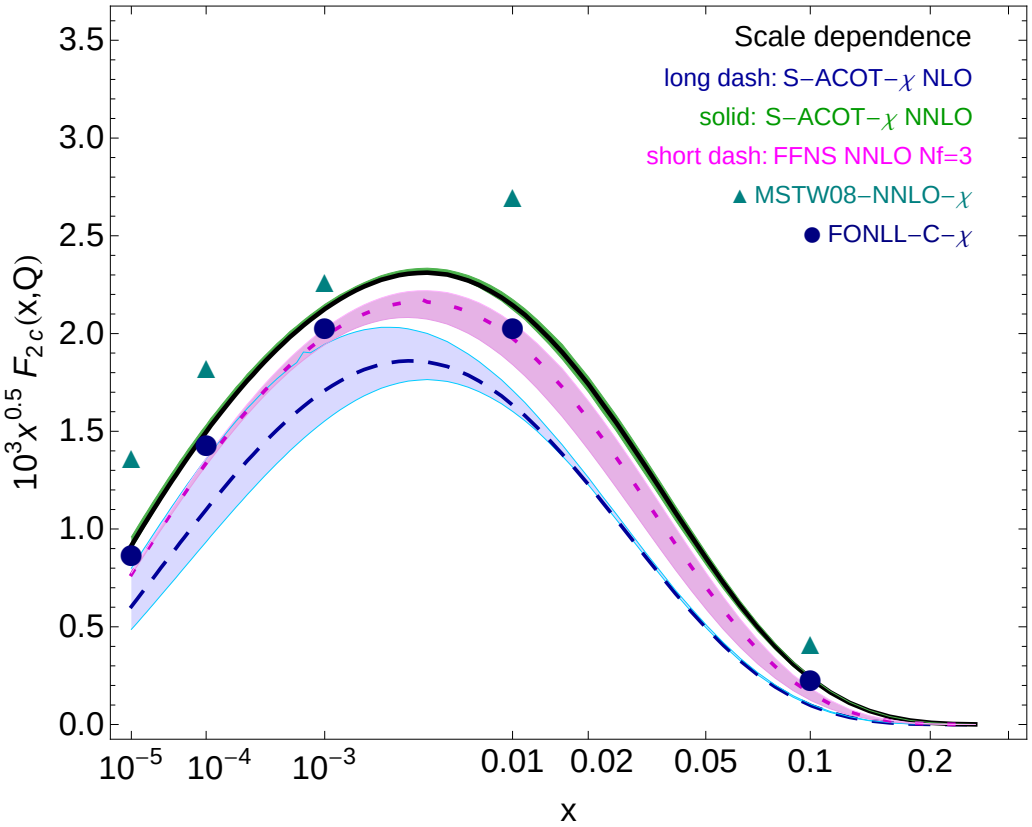

NNLO results for $F_2^{(c)}(x, Q^2)$

At NNLO and $Q \approx m_c$:

S-ACOT-χ $(N_f = 4) \approx$ FFN $(N_f = 3)$ **without tuning**

- S-ACOT is numerically close to other NNLO schemes
- NNLO expressions are close to the FONLL-C scheme

(Forte, Laenen, Nason, arXiv:1001.2312).

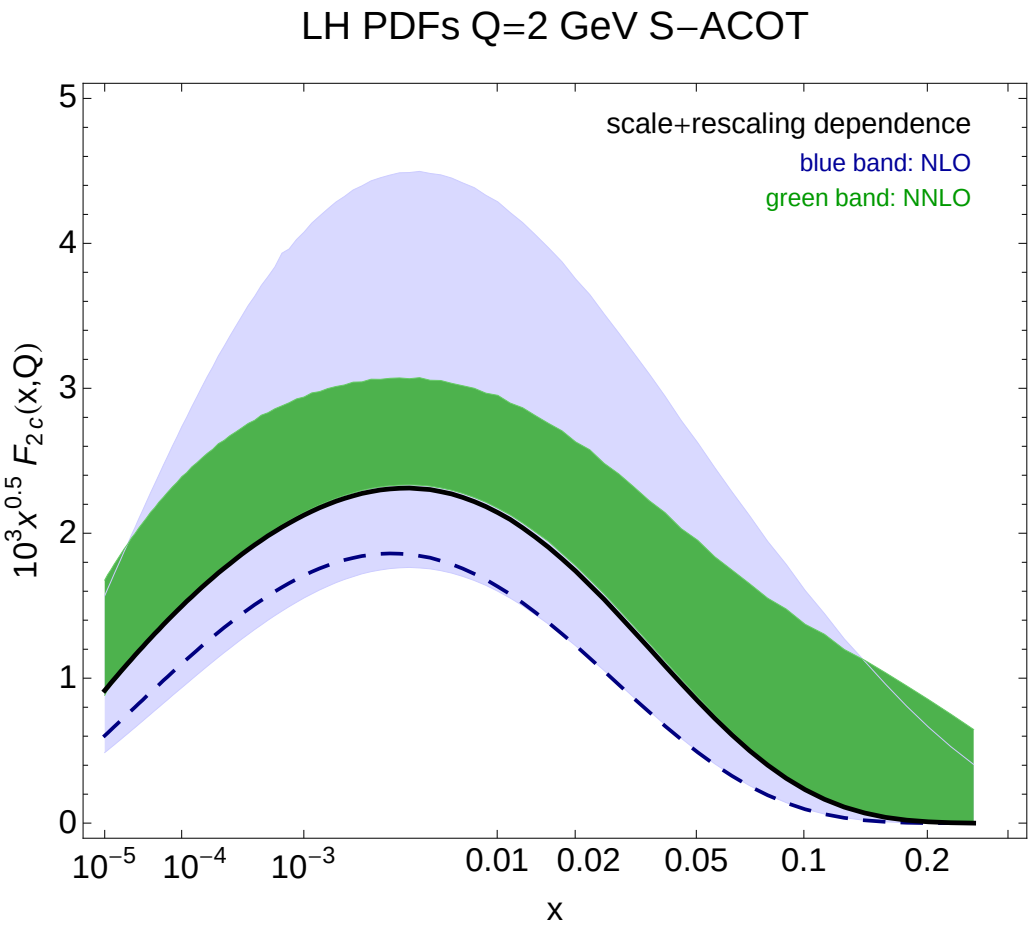

- Even without rescaling (**a wrong choice!**), NNLO cross sections are much closer to FFN at $Q \approx m_c$ than at NLO

Main features of the S-ACOT-χ scheme

- It is proved to all orders by the QCD factorization theorem for DIS *(Collins, 1998)*
- It is relatively simple
  - One value of N_f (and one PDF set) in each Q range
  - sets $m_h = 0$ in ME with incoming $h = c$ or b
  - matching to FFN is **implemented as a part of the QCD factorization theorem**
- **Universal** PDFs
- It reduces to the ZM $\overline{MS}$ scheme at $Q^2 \gg m_Q^2$, without additional renormalization
- It reduces to the FFN scheme at $Q^2 \approx m_Q^2$
  - has reduced dependence on tunable parameters at NNLO

CT10/CT10W distributions, W charge asymmetry, HERA DIS at small x

CT10 parton distribution functions (PRD82, 074024 (2010))

New experimental data, statistical methods, and parametrization forms

- combined HERA-1 data are included
- 53 CT10 and 53 CT10W eigenvector sets for $\alpha_s(M_Z) = 0.118$
- 4 CT10AS PDFs for $\alpha_s(M_Z) = 0.116 - 0.120$
  sufficient for computing the PDF+α_s uncertainty, as explained in PRD82,054021 (2010)
- CT10/CT10W PDFs with 3 and 4 active flavors
- **extended discussion of the Tevatron Run-2 W asymmetry data**
- **search for deviations from NLO DGLAP evolution in the small-x HERA data**

The puzzle of the W lepton asymmetry

- Rapidity asymmetry $A_\ell(y_\ell)$ of charged lepton $\ell = e$ or μ in W boson decay provides important constraints on $d(x,Q)/u(x,Q)$ at $x > 0.1$

$$A_\ell(y_\ell) = \frac{d\sigma(p\bar{p} \to (W^+ \to \ell^+\nu_\ell)X)/dy_\ell \; - \; d\sigma(p\bar{p} \to (W^- \to \ell^-\bar{\nu}_\ell)X)/dy_\ell}{d\sigma(p\bar{p} \to (W^+ \to \ell^+\nu_\ell)X)/dy_\ell \; + \; d\sigma(p\bar{p} \to (W^- \to \ell^-\bar{\nu}_\ell)X)/dy_\ell}.$$

- $A_\ell(y_\ell)$ is related to the boson-level asymmetry,

$$A_W(y_W) = \frac{d\sigma(pp \to W^+X)/dy_W - d\sigma(pp \to W^-X)/dy_W}{d\sigma(pp \to W^+X)/dy_W + d\sigma(pp \to W^-X)/dy_W},$$

  smeared by $W^\pm$ decay effects

Berger, Halzen, Kim, Willenbrock, PRD 40, 83 (1989); Martin, Roberts, Stirling, 1989

The puzzle of the CDF/D0 W lepton asymmetry

- CT10W set reasonably agrees with 3 $p_{T\ell}$ bins of $A_e(y_e)$ and one bin of $A_\mu(y_\mu)$ from D0 Run-2 (2008); shows tension with NMC, BCDMS $F_2^{p,d}(x,Q)$
- NNPDF 2.0 *(arXiv:1012.0836)* agrees with $A_\mu(y_\mu)$, disagrees with two p_{Te} bins of $A_e(y_e)$.
- CT10, many other PDFs fail.

Agreement of PQCD with D0 $A_e(y_e)$	χ^2/npt	Source or comments
CTEQ6.6, NLO	191/36=5.5	*Our study;* *Resbos, NNLL-NLO*
CT10W, NLO	**78/36=2.2** **With $A_\mu(y_\mu)$: 88/47=1.9**	
ABKM'09, NNLO	540/24=22.5	*Catani, Ferrera, Grazzini, JHEP 05, 006 (2010)*
MSTW'08, NNLO	205/24=8.6	
JR09VF, NNLO	113/24=4.7	

Why difficulties with fitting $A_\ell(y_\ell)$?

1. $A_\ell(y_\ell)$ is very sensitive to the average slope s_{du} of $d(x, M_W)/u(x, M_W)$

$$A_\ell(y_\ell) \sim A_\ell(y_W)|_{LO} \propto \frac{1}{x_1 - x_2}\left[\frac{d(x_1)}{u(x_1)} - \frac{d(x_2)}{u(x_2)}\right]; \quad x_{1,2} = \frac{Q}{\sqrt{s}} e^{\pm y_W}$$

Berger, Halzen, Kim, Willenbrock, PRD 40, 83 (1989); Martin, Stirling, Roberts, MPLA 4, 1135 (1989); PRD D50, 6734 (1994); Lai et al., PRD 51, 4763 (1995)

2. Constraints on s_{du} by fixed-target $F_2^d(x,Q)/F_2^p(x,Q)$ are affected by nuclear and higher-twist effects

Accardi, Christy, Keppel, Monaghan, Melnitchouk, Morfin, Owens, PRD 81, 034016 (2010)

Challenges with fitting $A_\ell(y_\ell)$

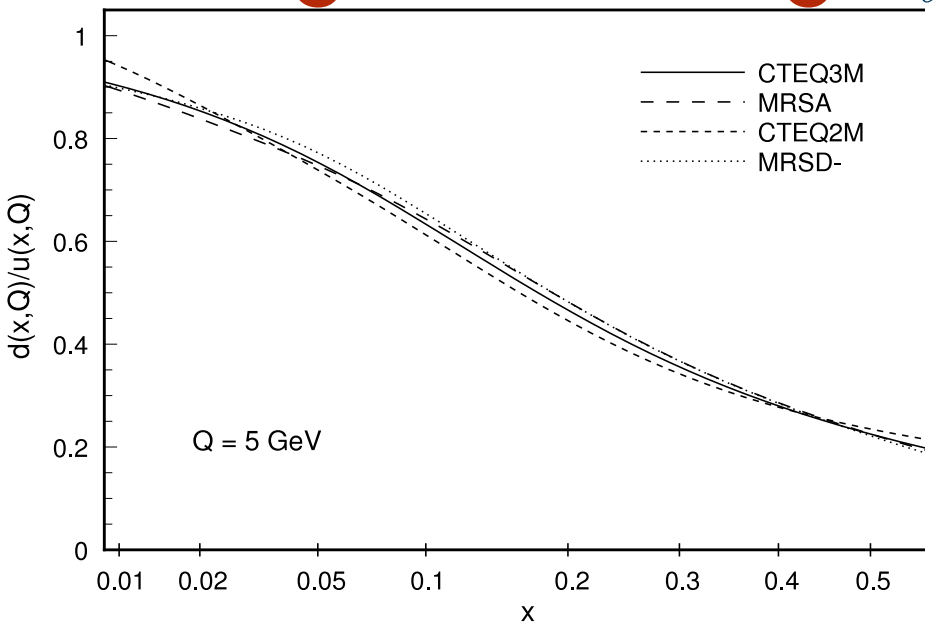

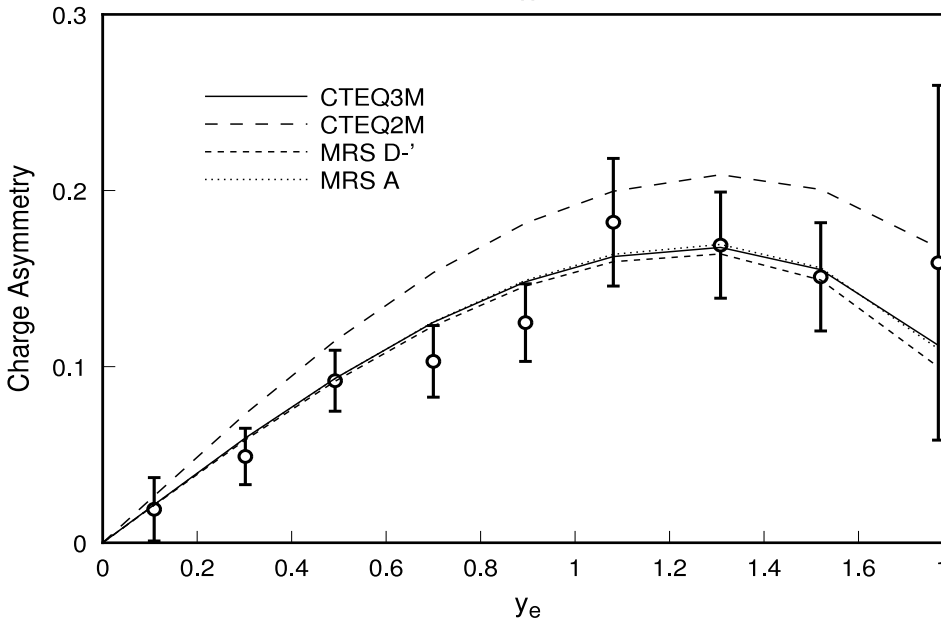

Small changes in s_{du} cause significant variations in A_ℓ

Lai et al., PRD 51, 4763 (1995)

Alternative constraints on d/u by $F_2^d(x,Q)/F_2^p(x,Q)$ from fixed-target DIS are affected by nuclear and higher-twist effects

Accardi, Christy, Keppel, Monaghan, Melnitchouk, Morfin, Owens, PRD 81, 034016 (2010)

$d(x,Q)/u(x,Q)$ at $Q = 85$ GeV

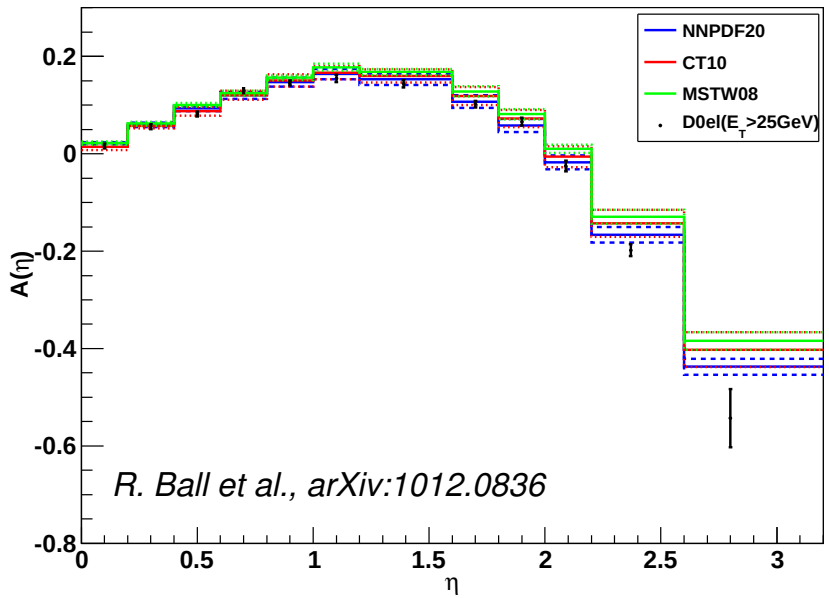

R. Ball et al., arXiv:1012.0836

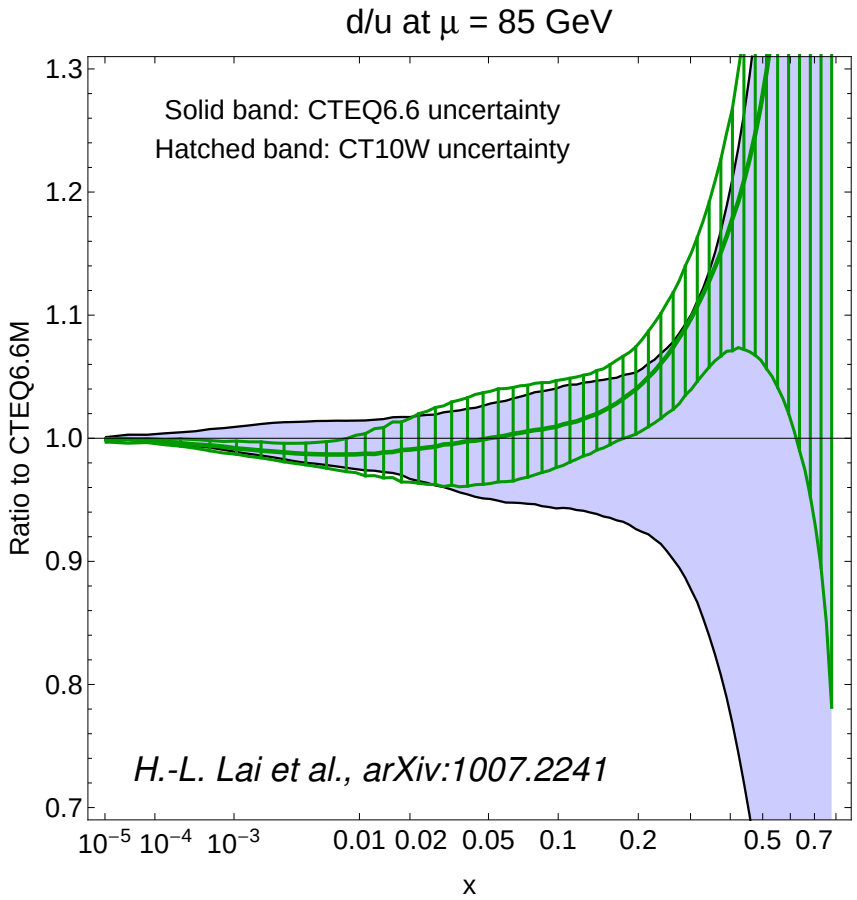

H.-L. Lai et al., arXiv:1007.2241

- D0 Run-2 A_ℓ data distinguishes between PDF models, reduces the PDF uncertainty

Why difficulties with fitting $A_\ell(y_\ell)$?

3. Existing parametrizations underestimate the PDF uncertainty on d/u

PDFs based on Chebyshov polynomials improve agreement with D0 Run-2 A_e, but are outside of current CTEQ/MSTW bands *(Pumplin)*

This ambiguity is reduced by $A_\ell(y_\ell)$ at the LHC, which constrains d/u and $\bar{d}/\bar{u}$ at $x \sim 0.01$.

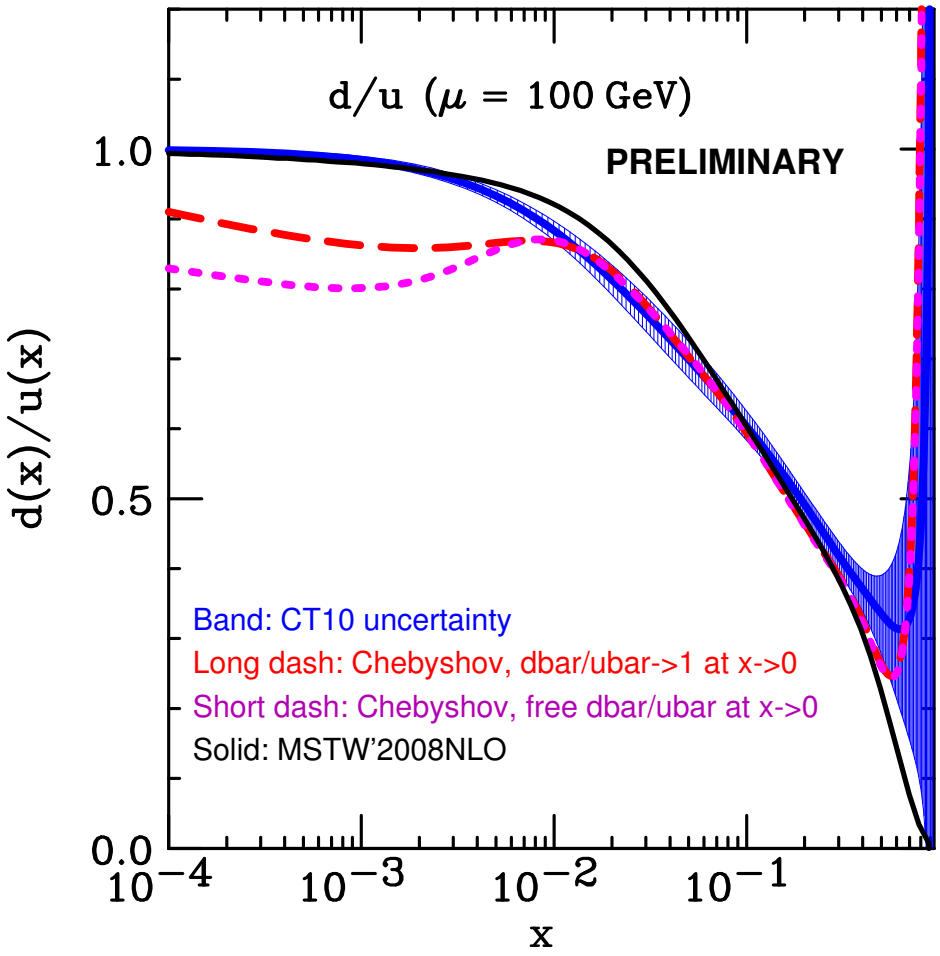

CT10(W) vs. A_ℓ at the LHC

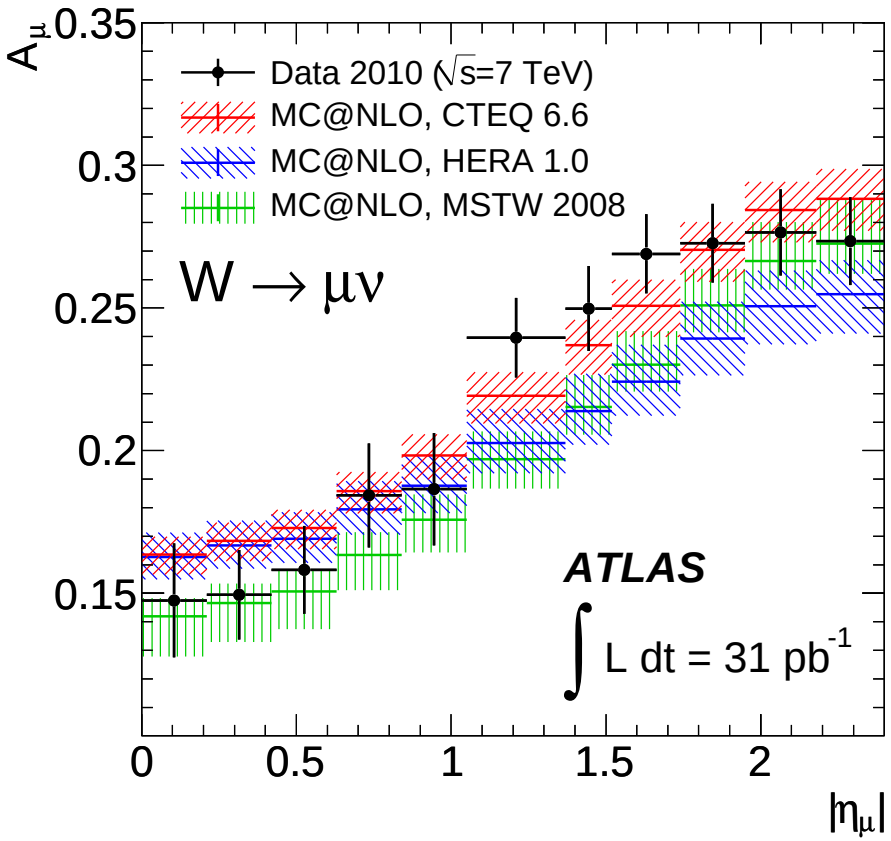

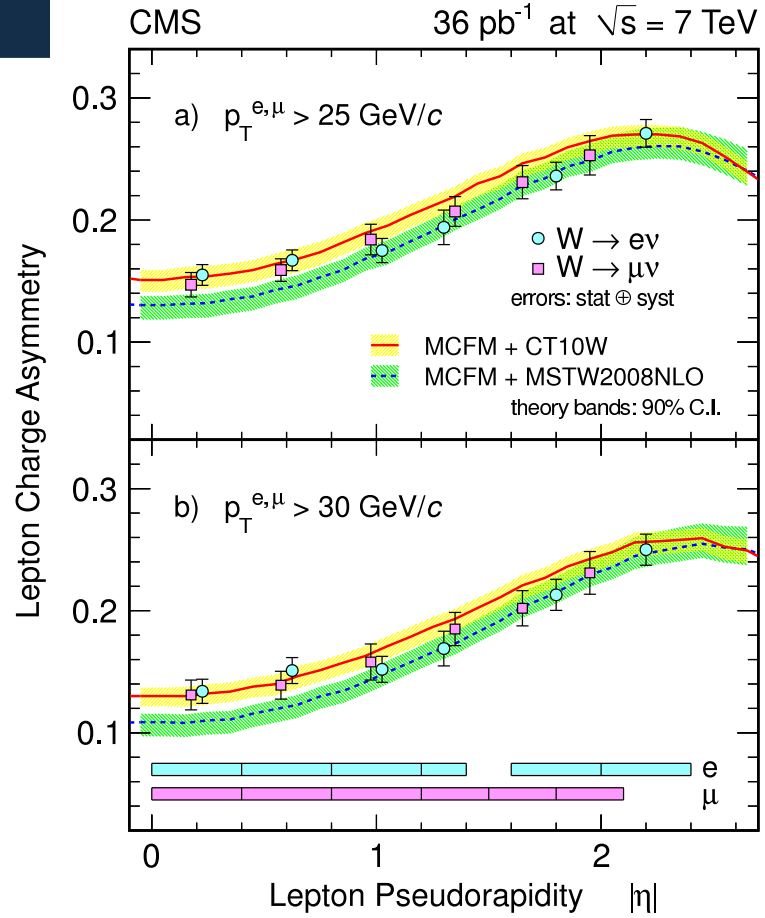

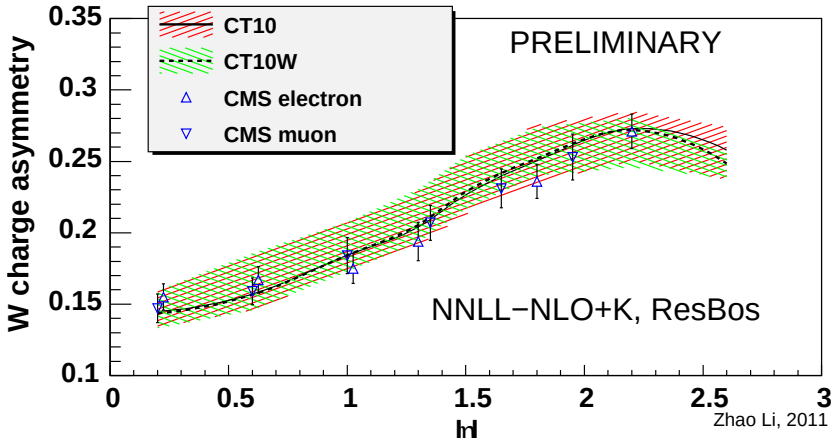

CT10(W) agrees well with the LHC A_ℓ; some differences between NLO and NNLL+NLO

CT10(W) vs. A_ℓ: LHC-B

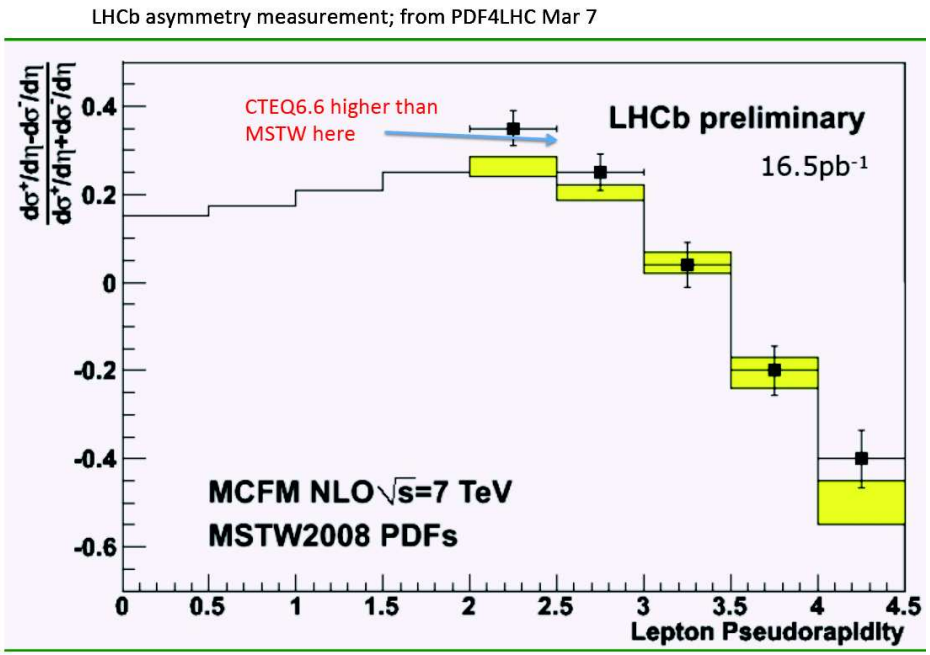

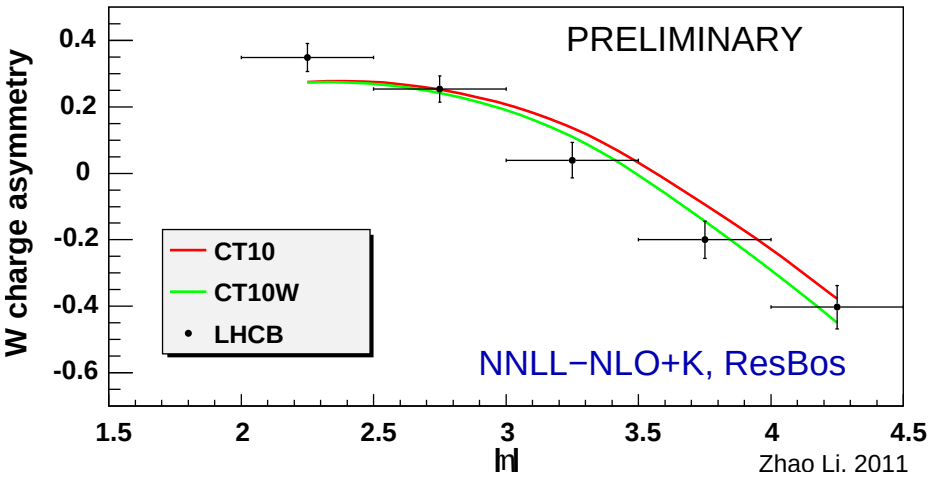

LHC-B marginally prefers CT10W

Why difficulties with fitting $A_\ell(y_\ell)$?

4. Experimental A_ℓ **with lepton** $p_{T\ell}$ **cuts** is sensitive to $d\sigma/dq_T$ of W boson at transverse momentum $q_T \to 0$.

- Fixed-order (N)NLO calculations (DYNNLO, FEWZ, MCFM,...) predict a wrong shape of $d\sigma/dq_T$ at $q_T \to 0$.
- Small-q_T resummation correctly predicts $d\sigma/dq_T$ in this limit.
- CT10(W) PDFs are fitted using a NNLL-NLO+K resummed prediction for A_ℓ (ResBos); **must not be used with fixed-order predictions for** A_ℓ.

For example:

$$\chi^2(\text{CT10W+ResBos}) = 1.9\, N_{pt} \text{ (us)};$$

$$\chi^2(\text{CT10W+DYNNLO}) = 8.4\, N_{pt} \text{ (NNPDF)}$$

Radiative contributions in ResBos + comparison to the Tevatron Z q_T distribution

- Resummed $d\sigma\left(pp \to (V \to \ell\bar{\ell}')X\right)/(d^3p_\ell d^3p_{\bar{\ell}'})$ for $V = \gamma^*, W, Z$, with decay and EW interference effects
- $Q_T \sim Q$: ($O(\alpha_s)$ with full decay) $\times$ (average $\mathcal{O}(\alpha_s^2)$ correction *(Arnold, Reno)*)
- $Q_T \ll Q$: $A^{(3)}$, $B^{(2)}$, $C^{(1)}$
  - no $H^{(2)}$ correction – a $\approx$ constant error of $\pm 3\%$ in the normalization of Xsecs
- mass dependence in c, b scattering cross sections *(S. Berge, P. N., F. I. Olness, hep-ph/0509023)*
- a nonperturbative function from *Konychev, P. N., hep-ph/0506225*

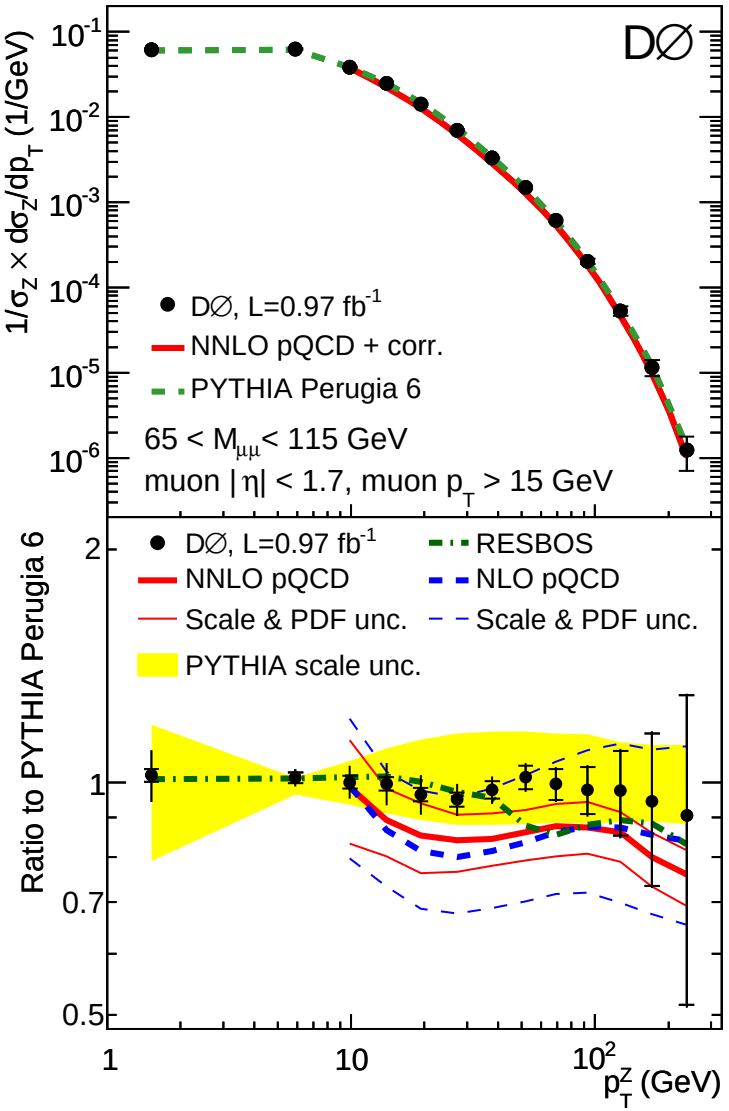

Charge asymmetry in p_T^e bins (CDF Run-2, 207 pb^{-1})

Without the p_T^e cut (FEWZ):

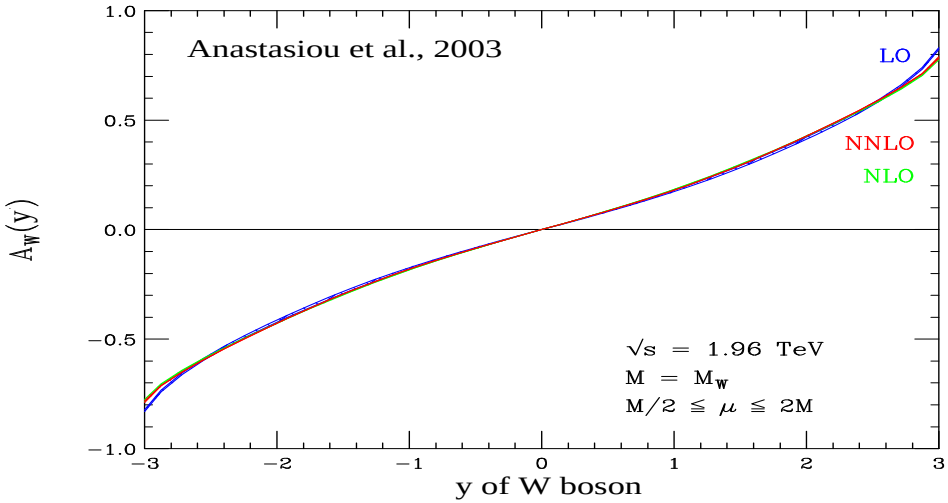

With p_{Te} cuts imposed, $A_{ch}(y_e)$ is sensitive to small-Q_T resummation

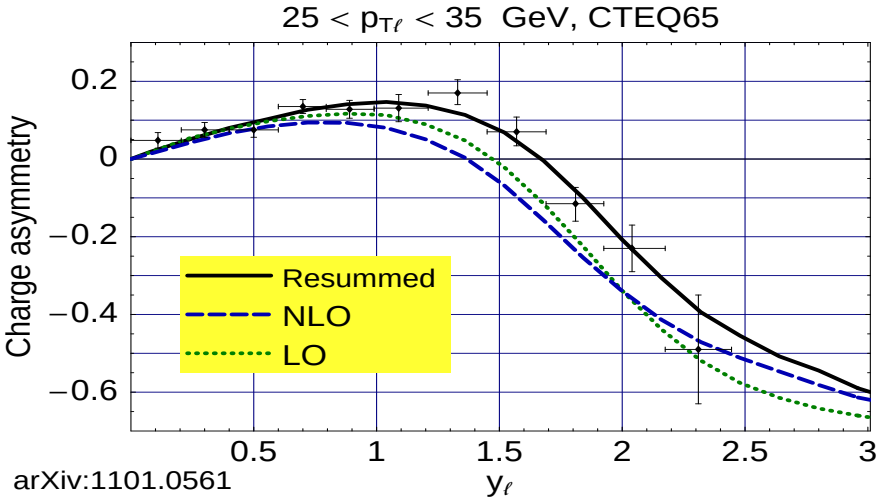

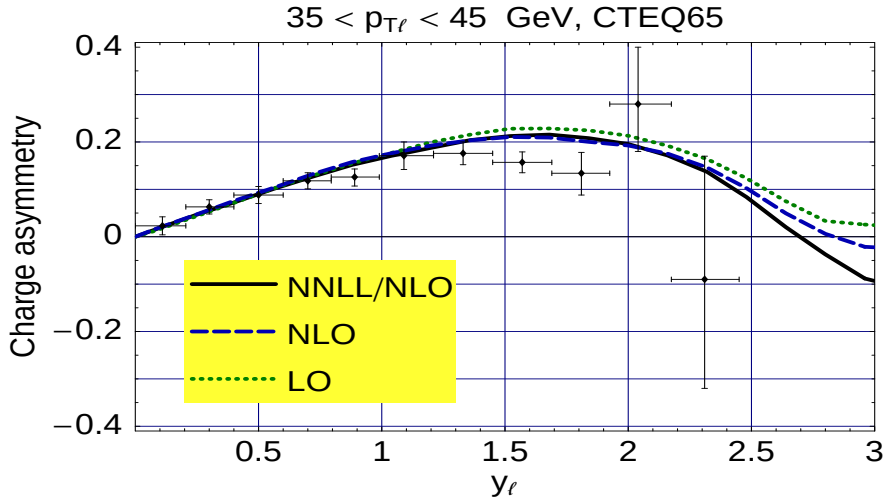

Balazs, Yuan, 1997; PN, 2007, unpublished; arXiv:1101.0561

A_{cut} fits to combined HERA data

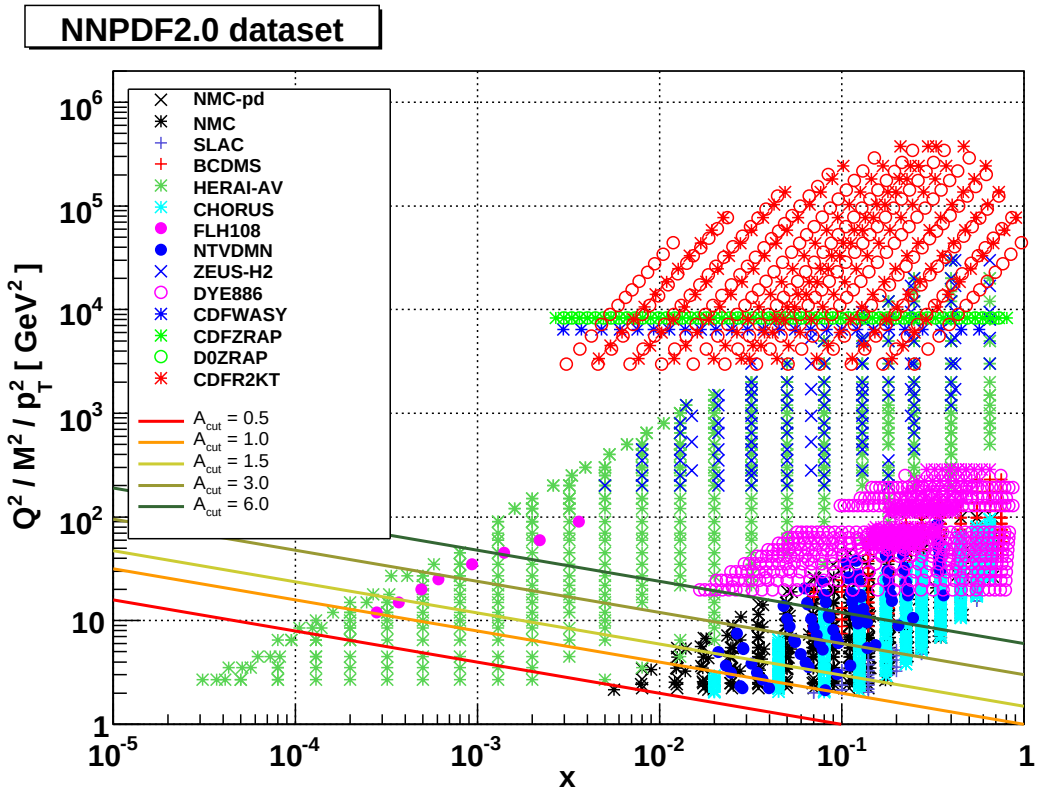

$$A_{gs} \equiv Q^2 x^{0.3} < A_{cut}$$

Fitting procedure:

- Include only DIS data above an A_{cut} line
- Compare the resulting PDFs with DIS data below the A_{cut} line, in a region that is "connected" by DGLAP evolution

CT10: A_{cut} fits to DIS data at $Q > Q_0 = 2$ GeV

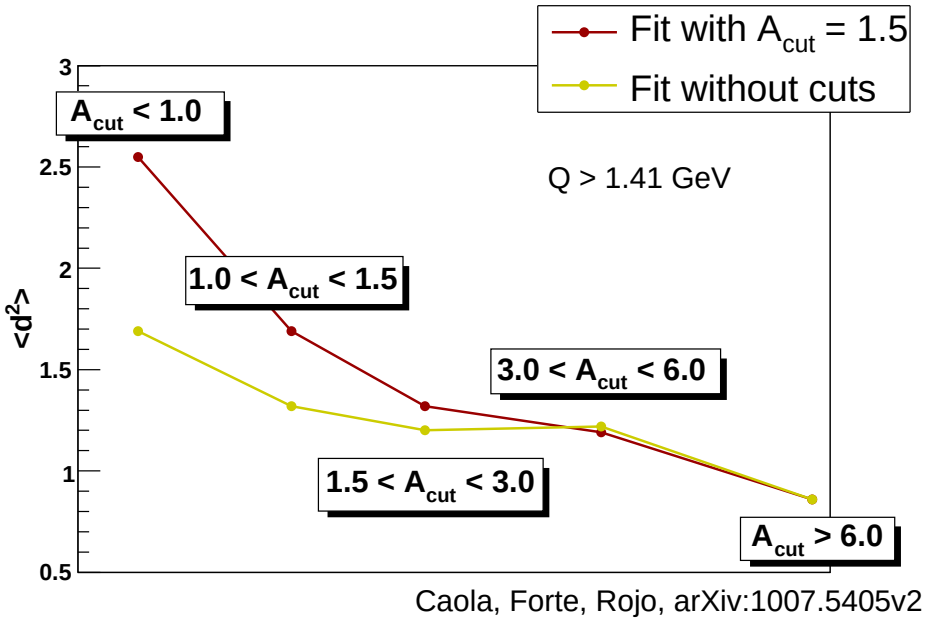

Caola, Forte, Rojo, arXiv:1007.5405v2

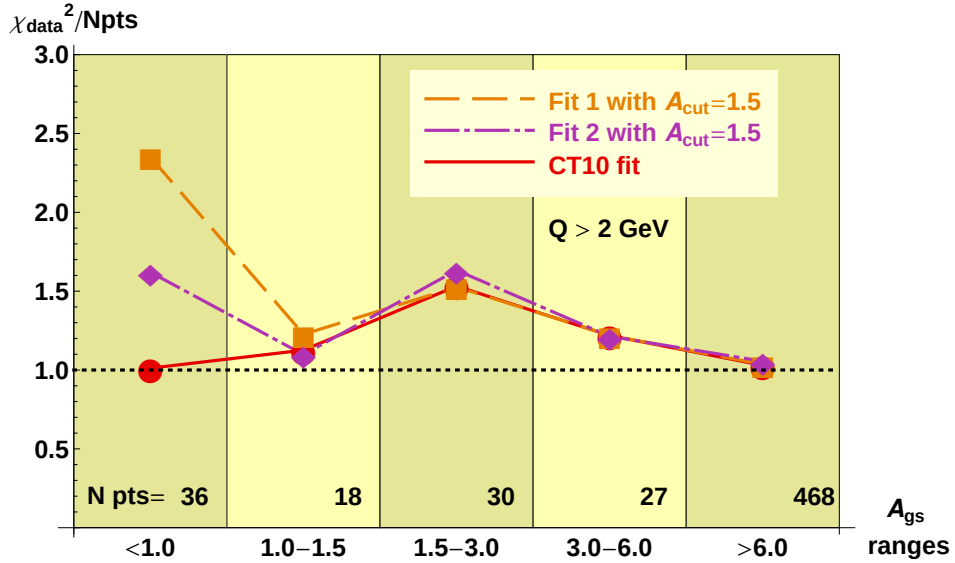

Motivation

Search for deviations from DGLAP evolution at smallest x and Q

- Follow the procedure proposed by NNPDF *(Caola, Forte, Rojo, arXiv:1007.5405)*

CT10: A_{cut} fits to DIS data at $Q > Q_0 = 2$ GeV

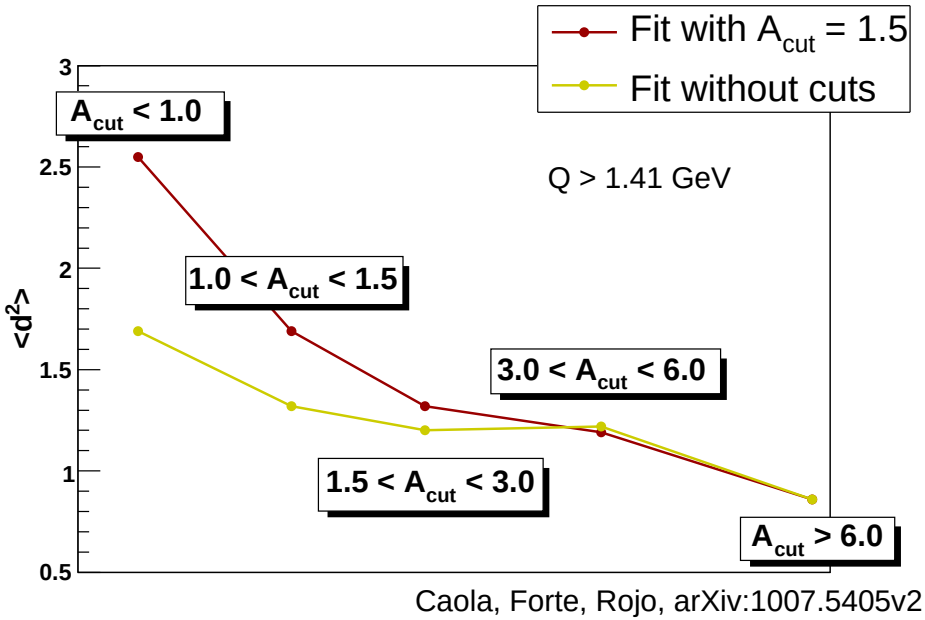

Caola, Forte, Rojo, arXiv:1007.5405v2

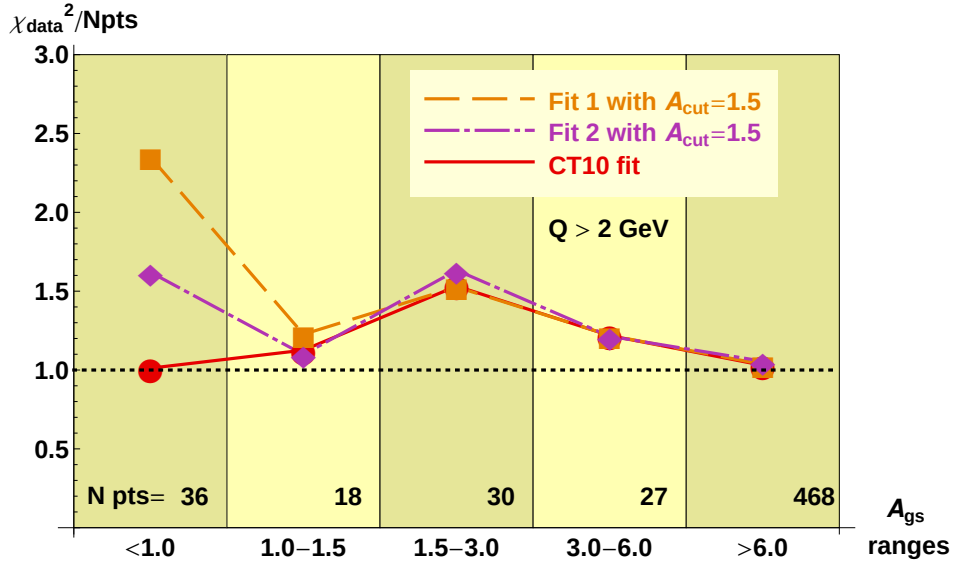

CT10

Two CT10-like fits to data at $A_{gs} > 1.5$, with different parametrizations of $g(x, Q)$

$$\chi^2_i = \frac{(\text{Shifted Data} - \text{Theory})^2}{\sigma^2_{uncor}}$$

Large syst. shifts at $A_{gs} < 1.0$, in a pattern that could mimic a slower Q^2 evolution

CT10: A_{cut} fits to DIS data at $Q > Q_0 = 2$ GeV

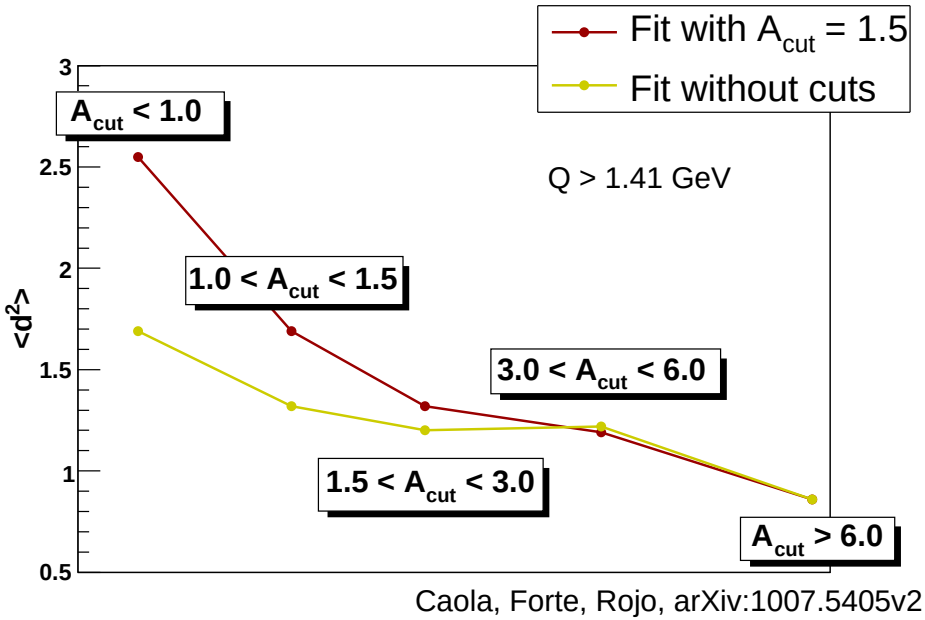

Caola, Forte, Rojo, arXiv:1007.5405v2

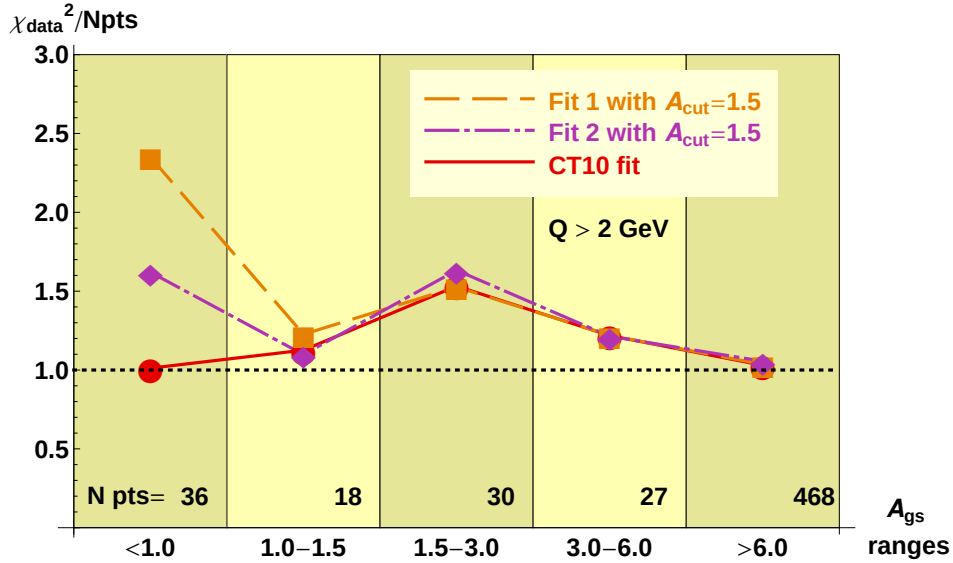

CT10, cont.

$\delta\chi^2 \sim 0$ at $A_{gs} > 1.0$
(no difference)

$\delta\chi^2 = 0 - 1.5$ at $A_{gs} < 1.0$,
with large uncertainty

$\Rightarrow$ Disagreement with the "DGLAP-connected" data at $A_{gs} < A_{cut}$ is not supported by the CT10 fit

Conclusions

- Great progress in understanding of heavy-quark contributions to DIS.
  - S-ACOT-χ recipe-like formulas for implementing NNLO
  - Energy conservation in DIS is realized as a part of the QCD factorization theorem. Would it be interesting to try to extend to pp processes.
  - It leads to rescaling of Wilson coefficient functions with incoming heavy quarks. The PDFs are given by universal operator matrix elements.
- Progress in understanding of NNLO contributions, new Tevatron and LHC data sets, PDF parametrization issues
- **arXiv:1101.0561**: synopsis of recent CTEQ publications
  - CT10W fit to Run-2 W charge asymmetry;
    PDFs for leading-order showering programs; constraints on color-octet fermions

Conclusion

Backup slides
1. Details on S-ACOT-χ scheme at NNLO

S-ACOT input parameters

At $Q \approx m_c$, F_2^c depends significantly on

1. **Charm mass:** $m_c = 1.3$ GeV in CT10
2. **Factorization scale:** $\mu = \sqrt{Q^2 + \kappa m_c^2}$; $\kappa = 1$ in CT10
3. **Rescaling variable** $\zeta(\lambda)$ for matching in $\gamma^* c$ channels
   (*Tung et al., hep-ph/0110247; Nadolsky, Tung, PRD79, 113014 (2009)*)

$$F_i(x,Q^2) = \sum_{a,b} \int_\zeta^1 \frac{d\xi}{\xi}\, f_a(\xi,\mu)\, C^a_{b,\lambda}\left(\frac{\zeta}{\xi}, \frac{Q}{\mu}, \frac{m_i}{\mu}\right)$$

$$x = \zeta \Big/ \left(1 + \zeta^\lambda \cdot (4m_c^2)/Q^2\right), \text{ with } 0 \le \lambda \lesssim 1$$

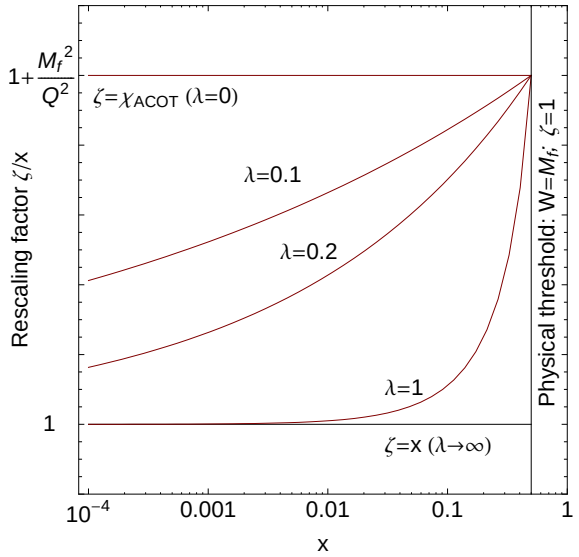

CT10 uses

$$\zeta(0) \equiv \chi \equiv x\left(1 + 4m_c^2/Q^2\right),$$

motivated by momentum conservation

Classes of Feynman diagrams I

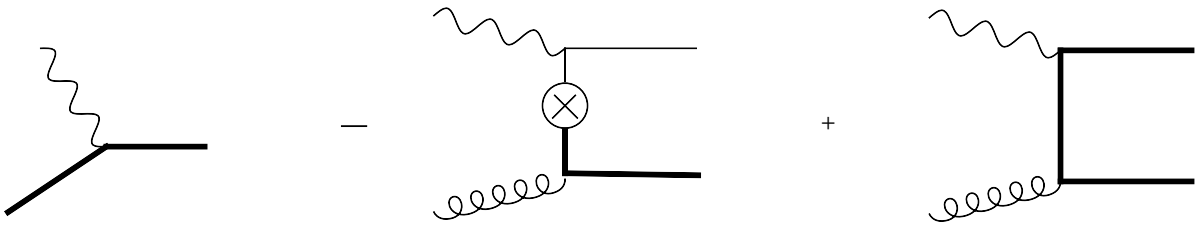

LO γ^* c — NLO Subtraction + NLO γ^* g

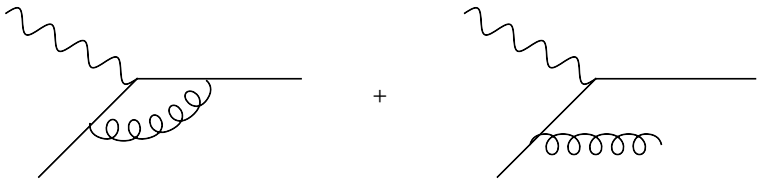

NLO γ^* c

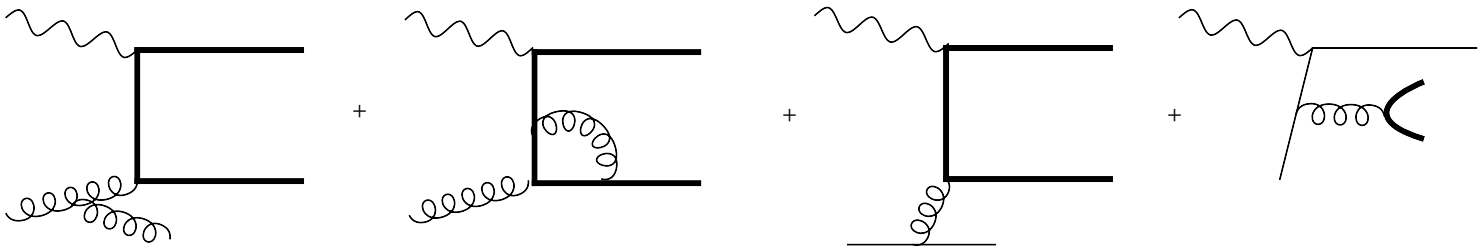

NNLO: γ^* g + NNLO: γ^* Σ + NNLO: γ^* q NS

Classes of Feynman Diagrams II

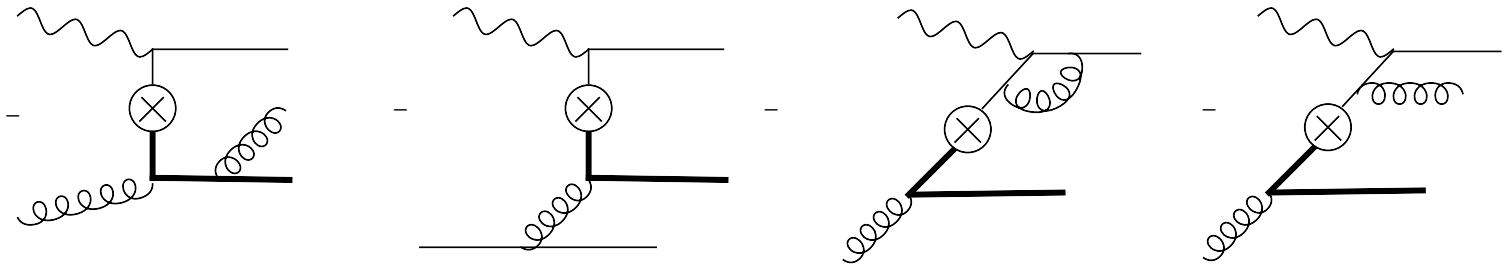

NNLO Subtractions

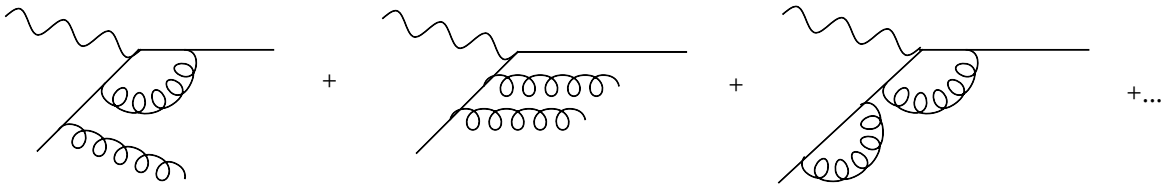

NNLO γ^* c

Cancellations between Feynman diagrams

Validity of the S-ACOT calculation was verified by checking for certain cancellations at $Q \approx m_c$ and $Q \gg m_c$

- $Q \approx m_c$:

$$D_{C1}^{(2)} \ll D_{C0}^{(2)} \ll D_{C0}^{(1)} \leq F_2^c(x,Q)$$

- $Q \gg m_c$:

$$D_g^{(2)} \ll D_g^{(1)} < F_2^c(x,Q)$$

These cancellations are indeed observed in our results

NNLO: Cancellations at $Q^2 \approx m_c^2$

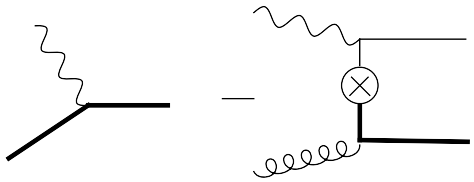

$$D_{C0}^{(1)} = C_Q^{(0)} \otimes c - a_s C_Q^{(0)} \otimes A_{Qg}^{(1)} \otimes g; \qquad a_s = \frac{\alpha_s}{(4\pi)} \tag{1}$$

$D_{C0}^{(1)}$

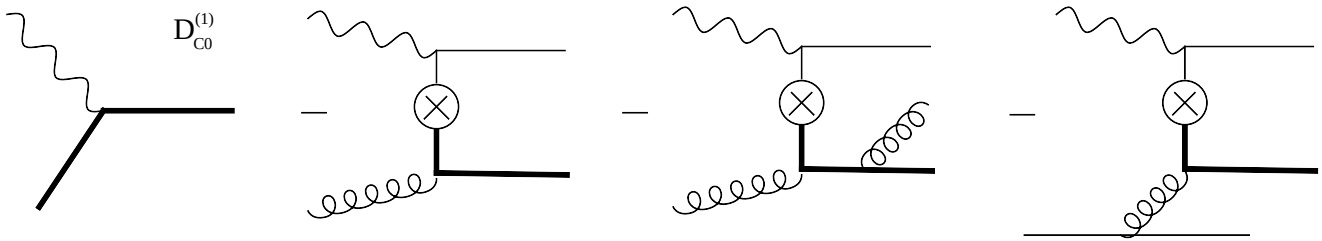

$D_{C0}^{(2)}$

$$D_{C0}^{(2)} = D_{C0}^{(1)} - a_s^2 C_Q^{(0)} \otimes A_{Qg}^{(2),S} \otimes g - a_s^2 C_Q^{(0)} \otimes A_{Q\Sigma}^{(2),PS} \otimes \Sigma \tag{2}$$

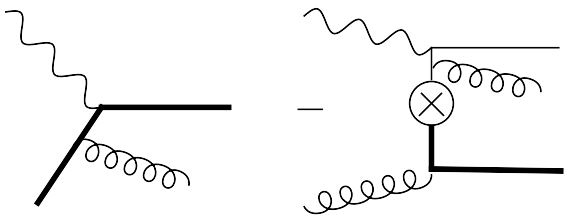

$$D_{C1}^{(2)} = C_Q^{(1)} \otimes c - a_s^2\, C_Q^{(1)} \otimes A_{Qg}^{(1)} \otimes g \tag{3}$$

$D_{C1}^{(2)}$

NNLO: Cancellations at $Q^2 \approx m_c^2$

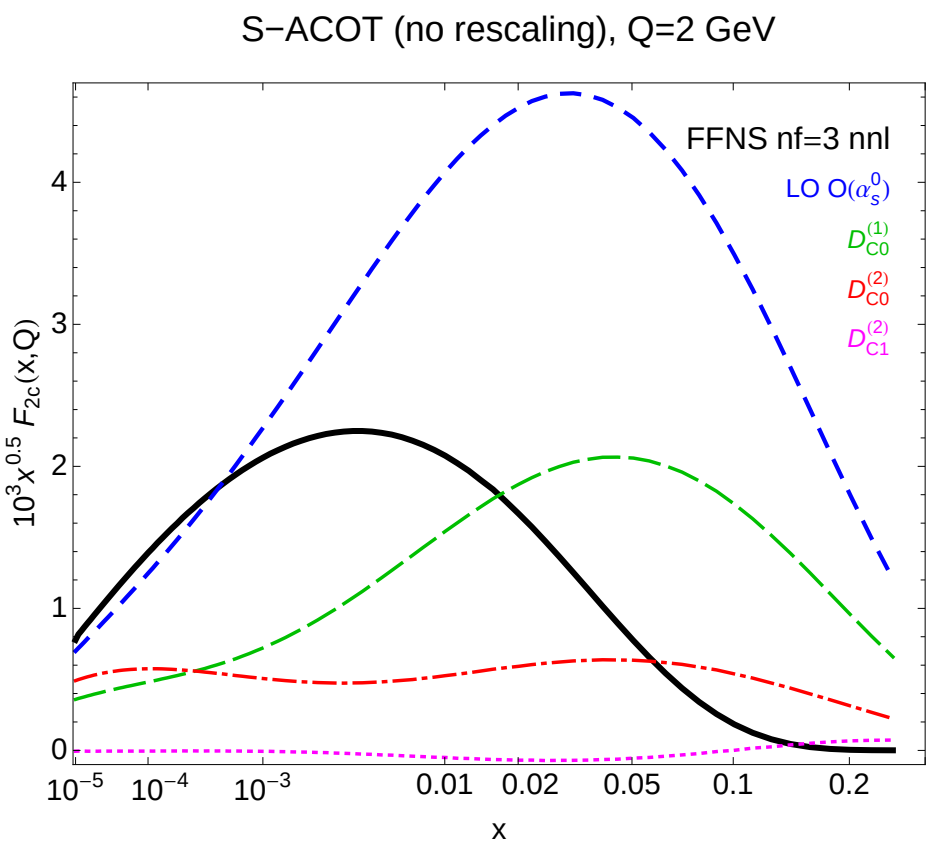

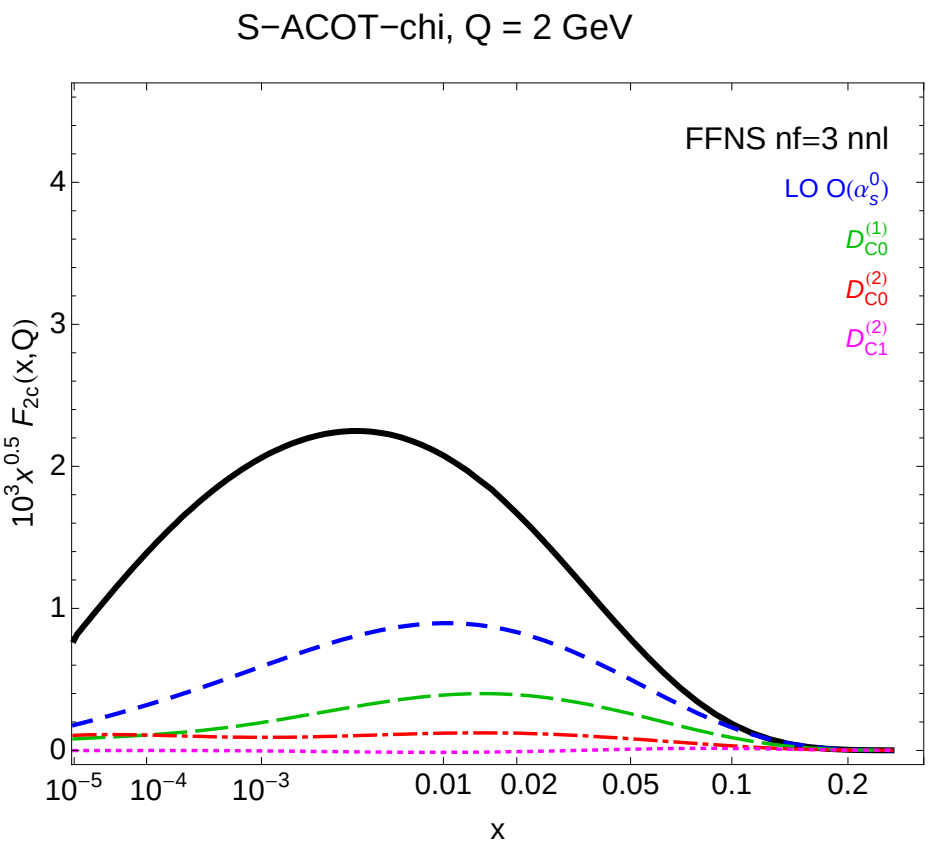

$D_{C1}^{(2)} \ll D_{C0}^{(2)} \ll D_{C0}^{(1)} \leq$ FFN at NNLO both for $\zeta = x$ and $\zeta = \chi$.

NNLO: Cancellations at $Q \gg m_c$

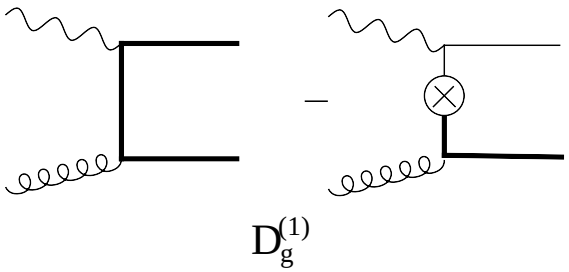

$$D_g^{(1)} \equiv C_g^{(1)} = a_s \left(F_g^{(1)} \otimes g - C_Q^{(0)} \otimes A_{Qg}^{(1),S} \otimes g \right) \tag{4}$$

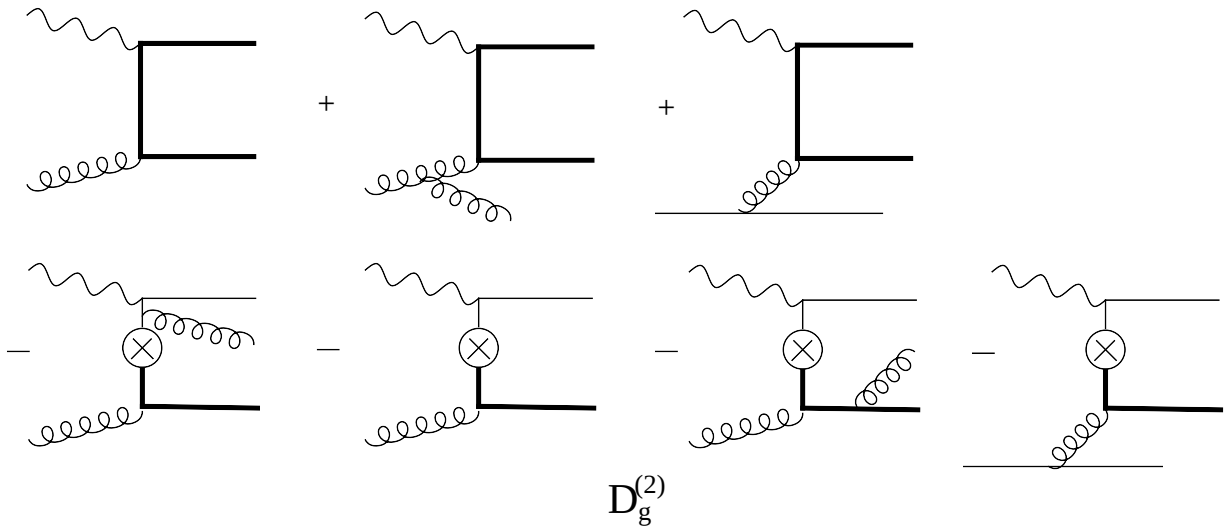

$$D_g^{(2)} = D_g^{(1)} + a_s^2 \Big[\tilde{F}_g^{(2)} \otimes g + \tilde{F}_\Sigma^{(2)} \otimes \Sigma - C_Q^{(1)} \otimes A_{Qg}^{(1),S} \otimes g$$
$$- C_Q^{(0)} \otimes A_{Qg}^{(2),S} \otimes g - C_Q^{(0)} \otimes A_{Q\Sigma}^{(2),PS} \otimes \Sigma \Big] \tag{5}$$

$D_g^{(1)}$ is of order of α_s^2 while $D_g^{(2)}$ is of order of α_s^3.

F_2^c at NNLO: Cancellations at $Q = 10$ GeV

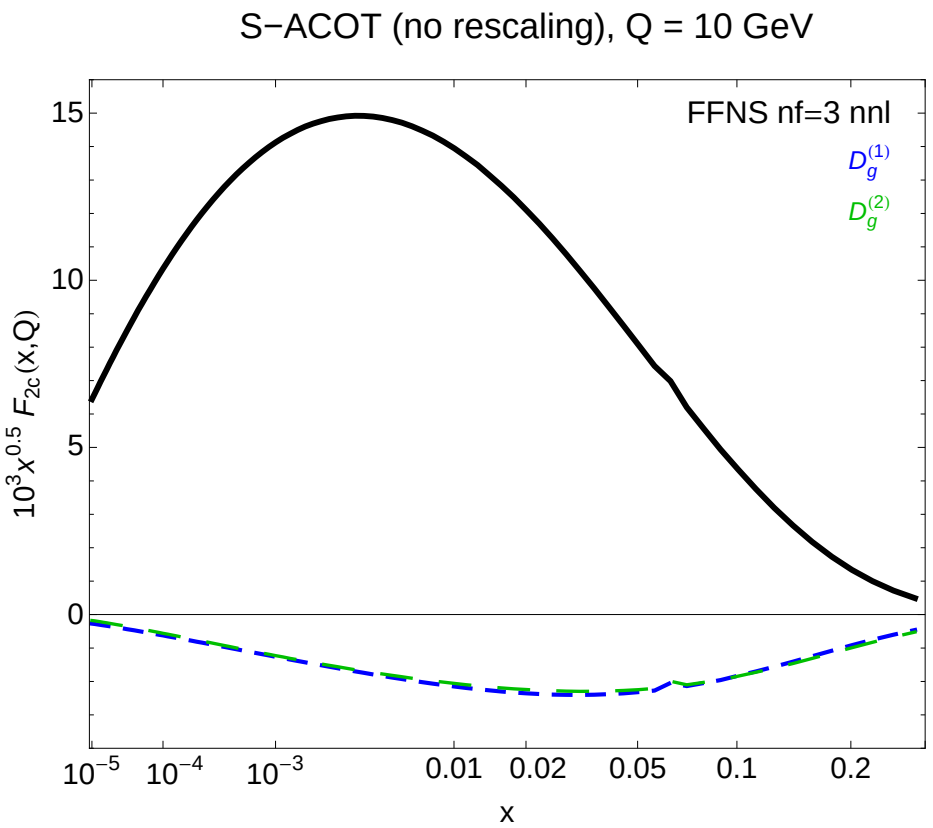

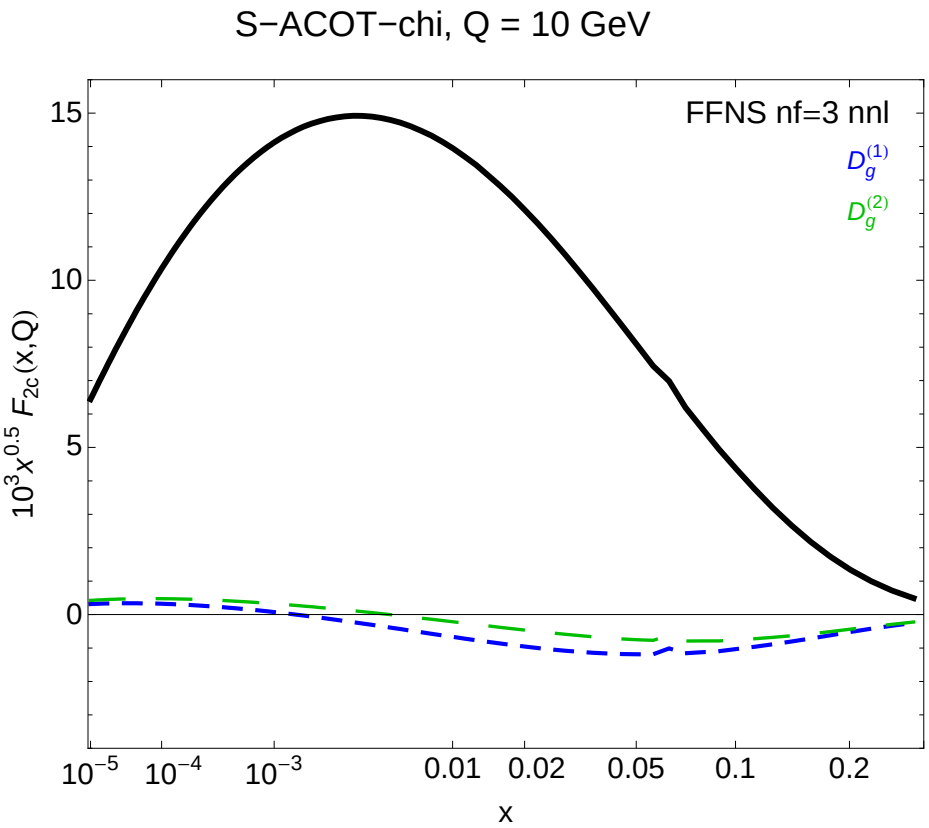

$D_g^{(2)} \ll D_g^{(1)} <$ FFN at NNLO $<$ ACOT

$\log \frac{Q^2}{m_c^2}$ terms in FFN are cancelled well by subtractions.

Comparison of (N)NLO PDF sets with data in the CT10.1 fit

- χ^2 are computed at NNLO, using the LHAPDF 5.8.6 interface and **CTEQ fitting code (very naively!)**
- Whenever possible, adjust settings to reproduce assumptions by other groups
  - Use $\alpha_s(M_z)$, $m_{c,b}$ values suggested by each PDF set
  - approximate the GM scheme in DIS if possible
- Correlated systematic errors are included according to the CTEQ method

$$\chi^2 = \sum_{e=\{\text{expt.}\}} \left[\sum_{k=1}^{N_{pt}} \frac{1}{s_k^2} \left(D_k - T_k - \sum_{\alpha=1}^{N_\lambda} \lambda_\alpha \beta_{k\alpha} \right)^2 + \sum_{\alpha=1}^{N_\lambda} \lambda_\alpha^2 \right]$$

- D_k and T_k are data and theory values $(k = 1, ..., N_{pt})$;
- s_k is the stat.+syst. uncorrelated error; λ_α are sources of syst. errors

χ^2 values per experiment (PRELIMINARY)

PDF set	Order	All expts.	Combined HERA-1	BCDMS $F_2^{p,d}$	CDF, D0 Run-2 1-jet	D0 Run-2 A_{ch}^{e}, $p_T^e > 25$ GeV
CT10.1	NLO	**1.11**	**1.17**	**1.10**	**1.33**	**3.72**
MSTW08	NLO	1.42 (1.28)	1.73 (1.4)	1.16 (1.17)	1.31	11.38
NNPDF2.0	NLO	1.37	1.32	1.28	1.57	**2.79**
CT10.2	NNLO	**1.13**	**1.12**	**1.14**	**1.23**	**2.59**
MSTW08	NNLO	1.34	1.36	**1.15**	1.38	9.84
NNPDF2.1	NNLO	1.57	1.36	1.30	1.51	5.45
ABM'09 (5f)	NNLO	1.65	1.4	1.49	2.63	**23.78**
HERA1.5	NNLO	1.71	**1.15**	**1.87**	**?**	5.4
N_{points}		2798	579	590	182	12